We thank the reviewer for their constructive comments that helped improve the manuscript. We provide an update of the manuscript with substantial revisions. These revisions include a shift of several sub-sections to the appendix.
In the revised manuscript (see attachement) we marked additions to the text in blue color and removed parts are red (except for many changes that just improved the language)

In the attached documents we address each reviewers' comments point-by-point.

Answer to RC1

General comments:
G.J. Schürmann et al., in their manuscript "Constraining a land surface model withmultiple observations by application of the MPI-Carbon Cycle Data Assimilation System", describe the MPI-CCDAS system, and a parameter optimization/state estimation experiment with it. The authors optimize various parameters of the JSBACH land surface model, utilizing remote sensed FAPAR data and CO2 flux measurement data from around the globe. They also analyze, how each dataset constrains carbon-related model variables, and what parameter values the MPI-CCDAS system optimizes the model to.
The topic at hand is important, since estimating the terrestrial carbon fluxes is difficult, and uncertainties in carbon stocks and fluxes are still large. Tuning a process based model makes it possible in principle to improve forecasts of how the terrestrial carbon stocks develop in the future.
There are several good things to say about the research at hand. For instance, the MPI-CCDAS is a new and seemingly useful tool for these kinds of experiments, and valuable in itself as a further development of the CCDAS system. The case study done with the system and presented in the manuscript is reasonable and the results generally seem to be good. The authors also nicely discuss and analyze why the results look as they do.
However, the manuscript is needs to be refined, expanded and clarified in some ways.
These are listed in the Specific comments section

Specific comments:
According to already the first sentence of the abstract, the paper is supposed to de-scribe the MPI-CCDAS system. However, the description of the system is unclear and there seems to be text missing between pages 2 and 3. Currently the section is written to vaguely describe that there is some data assimilation and some generic likelihood function being minimized. It would be important to include more specifics about the CCDAS method. What algorithm, how the data is used to update the state, when new parameter vectors are drawn etc. I'd enjoy explanations with formulas when needed. It would be also good to describe how the error covariance matrix for the likelihood function is constructed.
We apologize for the missing text. The missing text was:
„Technically, J is minimized through an iterative procedure using the Davidon-Fletcher-Powell algorithm in the Broyden-Fletcher-Goldfarb-Shanno variant in the implementation provided by the Numerical Recipes (Press et al., 1992, dfpmin routine). The required gradient $\partial J/\partial p$ is evaluated by the tangent-linear model …."
If fact, the missing text has probably obscured that the assimilation procedure is straight forward:
The minimised likelihood-function is given in Eq. 1. The assimilation procedure is given in the reference of the missing text and more details are given in Kaminski et al. (2013) and in reference therein. There is just one assimilation window with one set of control variables and one observational vector to be matched. We think Section 2.1 provides exactly the right level of detail on the methodology (which is a standard variational approach), with references to more elaborated descriptions. We have, however, added more explanatory text.

The differences of the parameter values obtained in Table 6 is large. They are discussed in the text, but there is no compact description of different error sources and their relative importances (like initial states, observation error, model bias, land cover type parametrization errors etc.). I understand that it was not the objective of this research to quantify uncertainties in the parameter and carbon stock values. Anyway, discussing the topic a bit more would be appreciated.
Currently we cannot assess the relative importance of the different error sources with our system.

Discussing these points would considerable lengthen the manuscript. The manuscript is already pretty long (as already mentioned by Reviewer 2). The focus of the manuscript should remain on the model description part. Nevertheless we already have some discussion of the topic in the outlook-section. This part will be extended to also name other potential reasons for uncertainties in the modelled carbon cycle components.
The extension reads as:
„Further assessing the relative importance of different error sources (e.g. in the land cover type parametrization, model biases or observational errors) with a system such as the MPI-CCDAS would allow to highlight priority areas to reduce their uncertainties and further constrain the global carbon cycle numbers as given in table 6).“

The language of the manuscript is not particularly good. Some sections are better than others. Very carefully checking grammar, breaking up too long sentences, checking capitalization rules etc. needs to be done. Some corrections are listed below, but they also could be wrong as I'm not a native speaker.
We have gone trough the manuscript and improved the language (without highlighting these changes).

There is a maybe a bit too much discussion-related content in "results", and some of it could go to the discussion part.
We checked for discussion related parts in the results section and moved this to the discussion which also helped removing some duplications in the text.

It is stated that the "prognostic capabilities of the model have been largely improved" (section 4.3) ... which is deduced from the two-year validation period. I'd like to believe that, but two years is not much. Could you please discuss this a bit further in the discussion part.
We refer here to the two year period which is also (in the layout of the experiment) a prognostic period. Hence for this two years the prognostic capabilities have been largely improved (reduced bias from 5.18 ppm to -0.05 ppm). We have not assessed longer periods (due to lack of data) and could only speculate on that. Thus we avoid opening a discussion on this topic.
To make the point clearer, we add a statement to the results section that we only refer to the 2 years period:
“In other words, the short-term (1-2 years) prognostic capabilities of the model have been largely improved for a 2 years horizon after assimilating CO2-observations, also at the evaluation locations.”

Technical corrections
section 1 / line 63: "certain processes..." is too unspecific. Please clarify.
These processes are the simulated phenolgy, and its seasonal and interannual climate sensitvity, as well as the simulated seasonal net land-atmosphere carbon flux. We added these details to the text:
“Dalmonech et al. (2015) have shown that the simulated phenolgy, and its seasonal and interannual climate sensitvity, as well as the simulated seasonal net land-atmosphere carbon flux are reasonably robust against climate biases in the MPI-ESM.”

s. 2.1 title: Phenology-module => The phenology module, or something
Changed to „The phenology module“

s. 2.2 / l. 61: what is "smoothly averaged temperature with a "memory"-time scale of 30 days"? There must be a more precise way of saying this.
This „smoothly averaged temperature“ is not representative for one single day or point in time. Rather it is the temporal average over the entire period with exponentially decaying weights with a

time scale of 30 days. The details are presented in the given reference.
We reformulate this to:
„The transition is controlled either by the length of the day t_d or a temporally averaged temperature T_m with exponentially decaying weights for older periods with a time scale of 30 days.“

sections 2.2-2.2.4 These sections are a bit long or unstructured somehow, as they describe just standrad JSBACH model physics. Particularly when compared to sections 2.2.5 and 2.1. More conciseness and clarity are needed.
The reason for giving this degree of detail is explained by the importance of the parameters for the CCDAS. In fact we only describe JSBACH-parts, where parameters have been taken from and some of the JSBACH parts are not standard JSBACH (the phenology). The reason for the shorter section 2.2.5 („Atmospheric transport“) and 2.1 („CCDAS-Method“) is, that they are described already elsewhere and that the details are not of importance for the optimized parameters.
In order to keep the details, we put these sections (2.2.1 – 2.2.4) to the appendix. To further improve readability, we also extended the description of the parameters in the main text with some more details (as suggested by Reviewer 2).

equation 5: Please state the mean and standard deviation of psi in the explanation, even though it looks obvious. As it reads, psi could be a distr with funny values.
We added the suggested clarification.

l. 75: "memory time-scale" (compare to "memory"-time scale earlier)... please be consistent and choose as comprehensible expression as possible
We corrected this

s. 2.2.2 / l 13: multiplication sign is not usually a star when printed. Use something like latex \times instead. Repeated many times in formulas, fix them all, please
We corrected this throughout the manuscript

l. 18 should it not be exemplified "by" instead of "for"?
We corrected this.

l. 20 ", gas" => ", and gas"
We corrected this.

sentence spanning the lines 29-39: restructure for readability
We restructured this sentence and it has gone to the appendix

equations 13,14,16: exp and min are not normally italicized in formulas
We changed this in the entire manuscript

s. 2.2.4/l.15 turns over to => turns to
We corrected this

s. 2.2.5/l.36- please clarify where "these" transport matrices refers to. The "responses" or what? I would not mind if this section was a bit expanded as well.
We did not explain TM3 in more detail, because this is standard TM3 and we do not optimize anything inside TM3. We compute the responses of the atmospheric CO2 concentration C to the fluxes F at the surface with the adjoint of TM3. The transport M itself is a linear process which leads to the formulation of $\Delta c=M*f$ and hence we refer to M as transport matrices. We add this formulation to the text. According to reviewer 2 we also moved some parts from the experimental

description to this section which gives further details about how we dealt with atmospheric transport.

2.3/51 why not say just "the assumed prior Gaussian uncertainty"?... and ...the posterior values from the assimilation experiments.
We changed this

Funny spacing in equations 20 & 21
We changed this

page 7, l. 15 "uncertainties...are based on expert knowledge" is quite subjective and ad-hoc. It's probably tricky, but I'd appreciate being more specific here. The expert knowledge has to be based on something, anyway. Please consider working on it.
All of these prior uncertainty estimates are not based on a formal uncertainty consideration, but rather on the authors interpretation of the recent literature. Q10 mainly is based on the experiences related to the work of Mahecha et al. (2010; Science). The uncertainty of f_aut_leaf is inspired by the sensitivity study of Knorr (2000; Global Ecology&Biogeography). For the initial uncertainties of the slow pool, we assumed arbitrary 10 % uncertainty, because we assumed no strong deviation from the equilibrium. For the CO2-offset we assumed only a change of a few ppm which led us to give the uncertainty of 3 ppm. This relatively large value allows a rather strong deviation from the prior without putting a strong penalty on the parameters. We added these clarifications to the manuscript.

l. 55 reference to EDGAR could go to references
This has been put to the references

s.4.1 / l. 69-72 the conclusion drawn is not immediately obvious to me, especially when "consistency" is not defined. I understand the basic idea here, but still, please clarify and explain.
The model can fit both data streams jointly and the costs sum up. In terms of a Bayesian optimization this is an indication that the model "fits" to the data-streams. The model is capable of reproducing the observed data streams without degrading other parts of the model (at least not those discussed in this part).
We moved this to the discussion where the arguments is getting clearer, because of a related discussion. This now reads as:
"The results clearly show that two data-streams can be successfully integrated with the MPI-CCDAS. The posterior parameter values (Table 2) were different between the FAPARalone and JOINT, as well as the CO2alone and JOINT experiments, showing that the joint use of the two data streams added information to the posterior parameter vector by preventing the degradation of the phenology simulation when trying to fit the CO 2 observations (Table 5 and 4). This is also supported by the fact that value of the cost function of the JOINT assimilation roughly equals the sum of the single data-stream experiments, indicating consistency of the model with both data streams."S

s. 4.1 /l. 85 norm of the gradient, but it's missing of what? costfunction? with respect to what? Please be more explicit here. It's possible to guess what you mean, but that should not be needed.
It is the norm of the gradient dJ/dp. We added this.

4.2/27 what is "magnitude of the phenological seasonal cycle"?
We mean here the average LAI. We clarified this in the text.

l.39 "For the other"... slightly odd sentence, please check
We clarified this sentence

p.12 l.14 f_photo => f_photos - usage not systematic in the text throughout it
We corrected this throughout the text

4.4.1/38 I read it as "an FAPAR" constant instead of "a"
This has been corrected

4.4.2/l57 C uptake , better maybe carbon uptake?
This has been changed in the entire manuscript

4.4.2/last sentence could be better formulated
We reformulated this

5.1/l.80 ranging from 111-151 => ranging from 111 to 151
We changed this

p. 15/l.1 References are quite old. Are there any newer ones available?
Unfortunately there are no more recent references on this

p.18/l.26 Northern extra-tropic => northern extra-tropical.
We have corrected this throughout the manuscript

Last paragraph of conclusions: first sentence quite long, please consider restructuring
We reformulated this

Answer to RC2

The paper describes a new carbon cycle data assimilation system based on the JSBACH land surface model and the assimilation of two major data streams: FAPAR and atmospheric CO2 concentrations (using TM3 model to relate surface fluxes to concentrations). The paper highlights the benefit of using the two data streams as well as their potential complementarity to constrain the carbon cycle. The study is relatively comprehensive and provides an honest description of the strength and weaknesses of the system. It is relatively new in the sense that it uses an advanced process-based land surface model that serves as the land surface component of an Earth System model. It provides some new insight on the potential of CCDAS and I thus recommend its publication in GMD. However, I have several comments and question as well as few recommendations that I would like to be taken into account to improve the manuscript. As a general remark the paper is quite long and there are several redundancies that could be avoided:

First i would suggest to put the detailed description of the model equations in an appendix with only a section in the main text that resumes the principles and highlights the main parameters. This is not mandatory but a suggestion.
We follow the suggestion here, especially because other reviewer also suggested a restructuring of the methods part. Section 2.2.1 to 2.2.4 (Detailed JSBACH description) have been moved to the appendix) and some more description of JSBACH and the relevant parameters have been added to the section on model parameters.

Sometime the discussion sections repeat the descriptions of the results in section 4, which could thus be avoided.
We agree with the reviewer. The duplication parts in the manuscript have been removed.

The conclusion seems could maybe be grouped with the outlook
In the outlook section, we express our opinion about promising further development of the CCDAS. We think it is work putting such a section into a manuscript that describes a model development and we also think that this content does not belong to conclusions. We thus have renamed this section to „Further development of the system“ and have merged some parts with the discussion to further streamline and shorten the text.

The selection of TIP-FAPAR data: I do not understand that the criteria to reject data (i.e. a prior correlation with the model output lower than 0.2) leads to disregard completely the temperate deciduous ecosystems (Europe, USA,. . .). Figure 1 reveals that mainly the boreal ecosystems and the tropical ones are kept. The result of such selection poses some questions that are important to discuss; The authors should mention how many PFT are kept after the selection and how many grid-cell are retained for each PFT as well as why the model behaves so badly for temperate ecosystems so that these grid cell are rejected. This is interesting as usually most LSM perform relatively well for deciduous temperate PFTs.
Here the reviewer misunderstood some parts. The temperate deciduous ecosystems are not omitted from the assimilation because they showed a poor correlation with the data, but as a result of the other selection criteria of omitting crop-dominated ecosystems: The temperate deciduous ecosystems for Europe and the US are collocated in grid-cells with a large fraction of crops. This leads to their omission. Because several PFT's occur in one grid-cell, it is not meaningful possible to summarize the reduction of PFT's in only a few numbers. We adapt the manuscript in section 2.4.2 to make this point clearer:
“First, owing to the fact that no specific crop-phenology is implemented in JSBACH, grid cells with fractional crop coverage of more than 20 % have been filtered out, as we cannot expect the model to fit cropland phenology. A consequence of this filter is to mask the deciduous broadleaf PFT in the

US and Europe, because in these areas, this PFT is collocated in crop-dominated pixels. Hence, the phenological parameters of the deciduous broadleaf PFT are only constrained by observations from other locations - a fact that should be kept in mind when interpreting the deciduous broadleaf parameters."

One important results concern the distribution of the net C terrestrial uptake. The larger sink in the northern high latitude compare to the other latitude bands (temperate around 40 ◦ N or the Tropics) is a strong feature of the MPI-CCDAS. The fact that suc sink occurs mainly in Siberia where the needle-leaf deciduous trees (Larix) dominate (East Siberia) can also be related to the fact that there are not many atmospheric stations around this area (except in the southern part). The differences in terms of NBP with the adjacent ecosystems (western part of Siberia) need to be discussed. To my mind this may be an artifact of the system and may not reflect the "true" distribution of the land carbon sink. Given the implication such spatial pattern may have for our understanding of the carbon cycle I suggest a stronger discussion of the potential weaknesses of the systems for the attribution of the net C flux; especially with a discussion of the "confidence" the author have in this partitioning. Section 4.4.2 describes the differences between the tests in these boreal regions but I think it should discuss more how "reliable" the main results are.

This description is perfectly in line with what the authors think about the East Siberian sink. We will state this clearer in section 4.4.2 where we added the following:

"This largely increased sink in Eastern Siberia could be an artefact of the set-up used for the data assimilation in this study. No nearby atmospheric stations constrains the net carbon sink in this region adequately, and the CD PFT only occurs dominantly in this region. In consequence, the PFT's parameters can not be adequately constrained by carbon cycle observations from other parts of the globe. This relative scarceness of observations and independency of other regions allows the East-Siberian net carbon uptake to compensate for other regions fluxes in order to match the global growth rate. Additional observations would be required to allow for spatially higher resolved estimation of the net fluxes."

SPECIFIC COMMENTS:

Method (section 2 and 3):

*** P2,L25-40: The paragraph mixes a review of data assimilation system based on different data stream and different methods. I would suggest to separate more the two issues (data and method). Also the review about the different data streams is not complete and misses studies that have assimilated satellite NDVI/fAPAR observations for example. The Luke (2011) PhD reference is not informative, as the data that are used are not mentioned.**

The paragraph was not intended to give an ample review on the assimilated data streams, more it was thought of method review while still mentioning the assimilated observations. We rewrite this paragraph to clearer separate aspects related to the method and to observations. We also refer to more works related to NDVI/FAPAR in the revised manuscript. Nevertheless a complete review on the topic of assimilating NDVI/FAPAR (or LAI) from satellite would deserve much more space then is available in this manuscript. Hence we keep it short.

Luke (2011) uses the MODIS collection 5 LAI product, see the paragraph with heading "MODIS LAI" in her section 6.4.1 (page 174).

***P2, L55-60: It would be clearer if the authors define what is the "original CCDAS" and clarify that CCDAS encompasses the assimilation of several data stream and not solely atmospheric observation.**

We refer to the BETHY-CCDAS (with a reference on the overview article of Kaminksi et al. 13).
We added this to the manuscript and state clearly that the CCDAS assimilates more then one data-stream.

*** P2, L55: The introduction should clearly mention the use of the two types of observations they are considered. The objectives and the questions that are posed do not reveal a major focus of the study: the complementarity of atmospheric CO2 and TIP-FAPAR data. This should definitely be presented in the introduction.**

We agree with the reviewer, that the complementarity of atmospheric CO2 and TIP-FAPAR is a major outcome of the study. Since this was not the primary intention of the work, we did not put this as an objective into the introduction. Nevertheless we add a short sentence to make this important point clear already in the introduction.

*** P2, L101-: The authors should provide briefly the principle of the "Davidon-Fletcher-Powell" algorithm (whether it needs and approximates the hessian of J).**

This algorithm approximates the Hessian of J. We added this clarification to the text:
"Technically, J is minimized by a quasi Newton approach with so-called Broyden-Fletcher-Goldfarb-Shanno (BFGS) updates of the Hessian approximation, in the implementation provided by the Numerical Recipes (Press et al., 1992, dfpmin routine)"

***P3, L25: "differentiable implementation of J(p)": This is not clear and I guess it is more a differentiable implement of some equation in the code but not of J(p) ?**

In fact, all code of the forward model that contributes to the calculation of J(p) needs to be differentiated. As long as the net-flux of CO2 is involved this requirement is met by almost the entire JSBACH-code. We clarified this in the text:
"The application of gradient-based minimisation procedures is facilitated by a differentiable calculation of J(p). According the the chain rule, this ultimately requires all code parts of the forward model that depend on the control variables and impact the cost-function to be differentiable.

***P3, L35: It is not clear what the author refers to with "through evaluation of sqrt(0) in the forward mode" ?**

The differentiation of a code with sqrt(0) leads in the differentiated code to 1/sqrt(0). We clarified this in the text:
"e.g. through differentiation of 0 in the forward mode leading to √ 1 0 in the diffentiated code"

*** P3 Equation 5: it would be good to precise the meaning of the different "control" parameters already in section 2.2.1 (and units), although the optimized one are described in Table 2**

We have moved the detailed JSBACH description into the appendix and added only a brief description of the model with a focus on the control parameters into the methods section.

***P4, L58: "PFT values are integrated. . .": which PFT values ? the GPP or the parameters?**

The PFT-dependent GPP is aggregated to a grid-cell GPP according to the fraction cover of each PFT. This is clarified in the text:
"GPP - values per PFT are integrated to grid-cell averages according to the cover fractions of each PFT within each grid-cell."

***P4, L77: how many layers has the soil water scheme?**

The soil layer scheme has 5 layers. This has been added to the description of the soil-scheme.

***P4, L83: It is not clear to which diffusion equation you refer to? (equation 15 ?)**

Yes it is equation 15. We add this reference to the text

***P5 section 2.2.5: There is no mention of biomass burning fluxes. The authors should justify**

why they have not also used an estimate of biomass burning as this may play a role especially for the trend at atmospheric station (given that the net biomass burning flux is roughly 1 PgC/year). The choice of only one constant offset for the atmospheric CO2 background poses the problem of the spin up of the atmospheric CO2 gradient. The authors should discuss this issue as it may significantly bias the parameter optimization. The mention later in section 3 that they use 2 years for spinning up the atmospheric gradients, which may be not enough. One way to address this issue is to mention if the simulated gradients after two years are relatively similar to the ones obtained after more years with the prior parameter sets.

We have not explicitly accounted for biomass burning fluxes and rather treat it as a respiratory flux. This can impose problems in the parameters optimisation, since this simplification may yield to compensating effects in the parameters estimates – especially because we only have a few degrees of freedom to adjust respiration, a fact well discussed as limitation in the manuscript. The alternative of adding the biomass burning fluxes as a background term (similar as fossil fuel and ocean carbon fluxes) introduces an inconsistency in the model, because the burnt carbon would need to be removed from the carbon stocks and post-fire dynamics would need to be accounted for. We already briefly discussed this issue in the manuscript but for this first application of the newly developed MPI-CCDAS we decided to focus on the most important processes and leave the inclusion of others to the further development. To make clear that we ignore the biomass burning fluxes, we add a statement about it to section 2.2.5:

“Biomass burning fluxes are not explicitly included (see also discussion in Sect. 5.6) and these fluxes are consequently mapped to the respiratory part of JSBACH during the assimilation of atmospheric CO2.”

The latitudinal gradient of CO2 is stable after one year of spin-up. The difference between Mauna Loa and South-Pole in January is 0.4 ppm and for the second year it reaches 4.8 ppm For the subsequent years it is variable (without a visible trend) within the range of 4.7 to 5.5 ppm. We added the following statement about this:

”After the second year, there is no visible trend in the difference of observed CO2 at Mauna Loa and South Pole. Thus 2 years are sufficient to spin-up the atmosphere”

***P7, L1: Why do you optimize only the size of the slow pool. You should justify with typical order of magnitude why the different litter pools are not considered (like with the mean residence time of each pool)**

The slow pool has a turn-over time-scale of 100 years where for example leaf litter has turn over times of a few years (depending on PFT). The reason for including only one modifier for the slow pool is mainly a computational one in order to limit the length of the parameter vector to be optimized. This is one of the main factors controlling the run-time of the system. We have chosen the slow-pool because it shows by far the longest turn-over time of 100 years, whereas for example the leaf litter has turn over times of a few years (depending on the PFT).

We admit that this might influence the estimation of the slow pool, since any discrepancies in any of the faster pools will be compensated by the slow pool. We added this clarification to the parameter description:

“For this first application of the MPI-CCDAS, the most slowly varying pool has been selected (i.e. the soil carbon pool with a turn-over time of 100 years). The initial conditions of other carbon pools were not included in the control vector to avoid the associated increase in the computational burden (e.g. run time). This consequently includes the risk of assigning any misrepresentation of modelled pools sizes to the soil carbon pool and the changes in the carbon pool sizes after the assimilation should be interpreted with care.”

***P7,L40: The paragraph on the description of TM3 should not be placed in this section which deals with atmospheric CO2. It should be in section 2.2.5. It is quite strange to mention the “fine grid” of TM3 given that it is at 4 by 5 degree resolution which is a very low resolution**

compared to existing studies and which thus may have an impact on how you can accurately simulate the spatial gradients between "continental stations".
Our initial intention was to put the TM3 description to the CO2 observation as an observational operator, because in principle any atmospheric transport model could be used to produce the matrices. But we agree with the reviewer, that it fits better to the description of the atmospheric transport. We also agree that 4 by 5 degrees is not a fine grid, but the TM3 naming is such that this grid is called „fine grid" and that is the reason why we mention this here.
We moved the TM3-description to the section about atmospheric transport.

***P7,L65-69: This discussion of the uncertainty in the FAPAR data does not touch the crucial point of potential biases. Indeed several previous studies (Kaminsky, 2012, Ba- cour 2015) have shown that FAPAR satellite data may be biased (because of different issues like saturation at high values,. . .) and that it is crucial to deal with these biases before any assimilation in a process-based model. This crucial issue should be at least discussed! I fear that if you would use a product with higher fAPAR values you would end up in very different estimate for the GPP and still a fit to both data stream.**
Yes there is saturation. It is, however, intrinsically addressed through the large uncertainty ranges over dense canopies. This is now clarified in the manuscript: "In this context we note that the per-pixel uncertainty ranges in the TIP-FAPAR product also reflect limitations of the information content that can be derived from sunlight reflected to space in the optical domain (i.e. the input to TIP) in particular over dense canopies."
We recall that the focus of this study was not to assess solely FAPAR as a data stream but the joint benefit of the data streams. We also discuss the issue of correcting for the bias in the prior model and observations and that this has a pronounced impact to the posterior GPP and respiration. Further we also clearly discuss, that GPP is not well constrained.

***P8,L13: It is confusing to mention the resolution of 8 x 10 here while in section 2.4.1 you mention the resolution of 4x5 for TM3. Please make it more clear between the two section to which resolution you effectively used TM3 and if you use the same resolution for JSBACH and TM3.**
We used 4x5 for the atmospheric transport, but 8x10 for JSBACH. We will make this point clearer.

Results (section 4)
***P 8, L66: should be the "cost function"**
This has been changed

***P9, L40: the sentence needs to be corrected.**
We reformulated that sentence

***P9, L39: Figure 2: This figure is not easy to read and I would suggest to decrease the number of year or to show only a mean seasonal cycle so that we could see more clearly the change in the timing of the model FAPAR.**
Since no relevant information is lost, we now only show 2 years of data.

***P9, L53, Figure 3: It would be more logic to plot in panel b: "Joint minus Prior" as you discuss the reduction of the LAI during the optimization.**
Thank you for pointing this out. We changed the sign of the plots and their title accordingly

***P11 section 4.3: Table 5: you should mention for the biases, which way it is: model – obs or the reverse.**
It is model – observations. This has been added to table 4 and 5

P11 section 4.3: As a general remark it is not easy from figures 4-5 and table 5 to see the improvement in terms of the phase of the seasonal cycle. I would suggest to calculate with the detrended time series a metric that reveal the phase changes, either the correlation or the length of the "carbon uptake period". This would complement the diagnostic of figure 5 on the mean amplitude.

A phase change in the atmospheric CO2 is hardly visible, which is the reason why we did not analyse it in more detail. At the monthly temporal resolution we apply here, we doubt that a metric for the phase change can be meaningful interpreted given that the change will be smaller then one month. Hence we decided not to add this diagnostic.

P13,L5: The change in the initial soil carbon pools, around 50% is huge and suggests that most of the global CO2 growth rate is matched by adjusting this unique scaling parameter. Although this is discussed later, it should be mentioned already that this will be discussed later as being a potential "limitation of the optimization set up".

We now mention, that this will be discussed later.

***P14, L30-34: sentence is too long and not clear. Need to be rewritten.**

We shortened this sentence to:

"Through the effect of net photosynthesis on canopy conductance (Eq. A14), the potential transpiration rate (E pot ; Eq. A5) was strongly decreased."

Discussion (section 5):

***P15L14-29 : This paragraph is not precise enough as for the "C in vegetation": whether you speak about above ground biomass, total biomass, soil C content,. . .. Please be more precise. The comparison to other estimates is interesting but you should have focus in such "discussion section" on a critical evaluation of what may be not accounted for in your model so that it could be pointless to try to be close to some independent biomass estimates. One potential bias is the steady state assumption for the vegetation so that the forest are mature while the "data driven" estimates of biomass account for the fact the most forest are relatively young compared to a mature forest. For the soil carbon the decrease by 50% of the prior initial soil carbon content lead to a value that compares favorably with the HWSD data. So this mean that the model itself tend to produce too much soil carbon or that the turnover of the soil carbon is not appropriated. These issues should be at least mentioned.**

Vegetation carbon in JSBACH is including carbon stored in all living parts of the vegetation above and below ground. The total carbon of the ecosystem is then the sum of this vegetation carbon, litter carbon and soil carbon. A more precise description of vegetation carbon is given in table 6 and the text.

We see some value in simply putting the modelled vegetation stocks (and their changes) in context to other estimates without a detailed discussion of the shortcomings of all the estimates.We decided to give the global number of all relevant stores and fluxes of the modelled global carbon cycle to allow for later comparison of our study with others, and also to allow identifying any major biases in the simulated global carbon cycle. We agree that a more in depth comparison of the different estimates would be desirable, but also agree with the reviewer that potential model shortcomings prevent such a close and in-depth evaluation.. We have not done this in the current work, because the focus was on the CCDAS model description and the implication of the data assimilation and not on the evaluation of the prior model itself, and potentially model biases that directly result from imperfections in the model formulation. We add the following note on this to the paragraph:

„A detailed comparison on the simulated vegetation and soil carbon stocks of the prior model is beyond the scope of this paper, partly because of the simplifications of the spin-up procedure entail biases in predicted vegetation carbon stocks, as transient land-use changes and forest management, affect-ing forest age structure are ignored. It is nevertheless instructive to provide context for the simulated vegetation and soil carbon stocks by comparing them to the global totals of independent

estimates.“

There is indeed a strong reduction in modelled soil carbon of JSBACH after the application of the MPI-CCDAS. But whether this means, that the prior model produces more carbon or whether the uncertainty of the HWDS data is too large to avoid such a conclusion is out of the scope of this manuscript. But since one of the main conclusions is, that the systems needs to be improved in terms of flexibility in constraining the respiration parts of the model, too much interpretation of the 50% reduction in soils stocks should be avoided.

***P15, section 5.2: last paragraph about the net carbon flux. You don’t mention the fact that your system neglected the net deforestation flux that would in principle add another C source to the atmosphere and would thus lead to a larger biosphere C uptake to balance the atmospheric CO2 growth rate. This should be at least raised as a caution when comparing to GCP estimates (or precise if you took for the GCP the net flux including deforestation).**
So far land use change emissions have not been accounted for in JSBACH. We have clearly discussed this in the outlook-section and similar reasons as for biomass burning fluxes (that imposing this flux would lead to inconsistencies with the stocks and fluxes simulated by JSBACH, as regrowth effects would have been ignored) led to the decision not to include this in the first MPI-CCDAS setup. We reported the „residual terrestrial sink“ of the GCP estimate, which does not include land use change emissions. We clarified these points in the manuscript.

***P15 section 5.2 first Paragraph: It would be interested to know whether the use of different spatial resolution with the JSBACH model may change or not the results.**
Yes this would be in fact interesting. But we have not conducted experiments with different resolutions and it was not the intention of this article to touch every unresolved point in applying a CCDAS. It was rather a systems description, that allows assessing these critical points in later works. Hence we do not feel capable of adding anything of substance about this point to the manuscript.

***P16 , L10-25: the discussion about the unique “Fslow” parameter could be a bit strengthened. First you should mention the additional cost (computation wise) that has prevented from the split of this parameter into several regions ? Also it would be interesting to see what the model provides in terms of soil carbon after a spin up with the new optimized parameters. How much the decrease in GPP lead to decrease the soil C content at equilibrium compared to the 50% requested decrease (through Fslow parameter) ?**
We refer here to the discussion in section 5.3.2, which covers this aspect. We disagree about the added value for giving initial soil carbon stocks computed with a posterior-parameter spin-up.
We clearly made the point in section 5.3.2 that this is a weak point of the current system and further discussing this point without improving on the shortcomings seems not appropriate.
We added the following statement about the run time to the discussion in section 5.3.2 „Parameter set-up“:
“This choice was made because allowing to control the spatial structure of the carbon pools would require several more parameters to be optimized, which would very likely suffer from a strong equifinality problem, and which would considerably extend the already lengthy run-time of the MPI- CCDAS”

***P16, L27: the conclusion that a better estimate of GPP in the tropic with additional constraint will likely improve the net CO2 flux is not obvious. As you say above the constraint on the net C flux does not lead to a direct constraint on GPP so the reverse is probably the same. Else the authors should detail the argument.**

Our argument refers to both, GPP and ecosystem respiration (the gross fluxes). Once these two fluxes in the tropics are well constrained, this also counts for the net-flux. A well-constrained tropical net flux will have beneficial impact on the estimation of the global net fluxes. We clarify that we refer to GPP and respiration.

***P16, last Paragraph of section 5.2: I found the discussion about the NPP not very informative for a general audience and I would suggest to drop it, given the current length of the paper.**
We agree that one could skip this paragraph. We follow the suggestion of the reviewer and delete this paragraph.

***P16, section 5.3, first paragraph: The first sentence is difficult to understand? Please consider rewriting; Line 60: it is not clear what the "alternative method" refers to?**
See the following comment.

***P16: Overall section 5.3 is not really informative and does not really provide a critical appraisal of the current MPI-CCDAS (the title). I would either just drop it, or discuss more fundamental issues due to the resolution of the transport model, the limited set of parameters (like Fslow), the restricted coverage of FAPAR data, the key potential limitation of the system to fully "model/explain" the net carbon fluxes (biomass burning, N cycle, land use change, forest age, ...).**
We follow here the suggestion in the next comment to largely drop this section. Parts of it are included in the outlook section

***P16, L85-90: I disagree with the argument that using a sequential design for as- similating several data streams leads by principle to a different result than using a simultaneous approach. Theoretically the Bayesian theorem could be recast in terms of conjunction or multiplication of probabilities so that it could be equivalent to use a sequential or simultaneous approach, provided that you can carry all the information about the parameter PDF from one step to the next. However, the practical implementation of the optimization system (such as for instance the use of Gaussian errors, the inability to calculate fully the whole PDFs,. . ..) generally lead to differences between the two approaches but it is quite difficult to fully establish which one is superior as you may also have "some benefits" of not exposing certain parameters to certain data streams in a sequential approach. I thus strongly recommend to rewrite this part in order to clearly state that the difference comes from the implementation of the CCDAS rather than from a theoretical point of view.**
We may have formulated our argument too strictly but we still think that our argument is valid and gives important insight in how to set up an assimilation system. If one would be able to compute to full posterior PDF (propability density function), the underlying model likely is computationally as fast that it is not necessary to employ a tangent-linear assimilation procedure, but one could chose a more costly algorithm (like e.g. MCMC; Monte Carlo Markov chain). Further, the need to implement a sequential design (sequentially in the order of the ingestion of the data streams, not sequential in time as is the case for e.g. Kalman filters) often comes with limiting the parameter vector for the one or the other data stream. In doing so, the linkages between parameters is broken (you cannot propagate information to a parameter that is not optimized in one of the steps of the sequential approach). Our example points towards problems with such implementations and we think it is worth leaving this part of the discussion in the manuscript. As the reviewer suggests, we reformulate this paragraph to make this point clearer:
"An implementa-
tion of such a sequential assimilation likely reduces the number of parameters to be optimized in each step, and therefore allows a quicker solution of the optimisation problem. However, this advantage comes with the cost of breaking the linkage between parameters can lead to situations, where the posteriori results of a sequential assimilation experiment will not match the observations

equally well as with a simultaneous assimilation."

***P16-17, Section 5.3.1 last paragraph: there is some redundancy concerning the gradient of the cost function not approaching zero for CO2 data with the same description in section 4.1, second paragraph. To decrease a bit the length of the paper it could be good to avoid repetition between these two paragraphs. But more importantly I fear that the proposed tests are not really going to help resolving this issue, as it is most likely due to a "minimization problem" related to the computation of an accurate gradient of the cost function or to limitation of the chosen algorithm in specific non linear circumstances.**

We further agree with the reviewer that the proposed tests are not solely to resolve this issue but also will shed light to other questions regarding the application of a CCDAS.

We removed the redundancy in the results section since it seems more appropriate in the discussion and we added the reviewers idea of how to assess this problem to the text:

"Investigation of the non-linear nature and potential numerical issues regarding the computation of the gradient $\partial J / \partial p$ (Eq. 1) might be needed. Further tests with alternative station network settings, parameter priors or time-periods will provide more insight into approaches to tackle this issue."

***P17, section 5.3.2, second paragraph: As mentioned above it would be good to dis- cuss here the value of the soil carbon content following a spin up performed with the optimized parameters to see how much of the decrease would arise from lower GPP. Potentially the discussion on this initial C pool scalar that occurs in several place in the paper could be group in this section (a suggestion).**

We refer here to the discussion above and consequently do not add the number of the carbon pools

***P17 section 5.3.2, last paragraph: the discussion on the "reduced prior estimate for the coniferous evergreen PFT" (L74) is not easy to follow. You should precise that the reduce prior estimate concerns the maximum foliar area in this sentence. I think that this pertain more to the method section and does not need a whole paragraph.**

Basically we agree with the reviewer that this paragraph belongs more to the method sections. There the reduction of prior LAI already is mentioned and hence we omit this paragraph.

Answer to RC3

Authors describe the assimilation of FPAR and atmospheric CO2 data into the MPI- CCDAS framework and the paper concludes that the assimilation of these two pieces of information allow to tune parameters of the terrestrial ecosystem component so that it performs better after it runs unconstrained.

The manuscript is interesting and GMD is a proper avenue for its publication but in its current format the manuscript is too long, or it appears too long because of its arduous reading since several points are not clear. The framework is not very well described so a reader is left to wonder.

If fact, a missing bit of text has probably obscured that the assimilation procedure is straight forward. We are very sorry for that. The missing text was:

„Technically, J is minimized through an iterative procedure using the Davidon-Fletcher-Powell algorithm in the Broyden-Fletcher-Goldfarb-Shanno variant in the implementation provided by the Numerical Recipes (Press et al., 1992, dfpmin routine). The required gradient $\partial J/\partial p$ is evaluated by the tangent-linear model ….“

We think Section 2.1 provides exactly the right level of detail on the methodology (which is a standard variational approach), with references to more elaborated descriptions. Unfortunately the missing text (see later) included some parts of the description of the framework. We also added more details to further describe the system. To reduce the length of the manuscript, we have moved the model description to the Appendix. We have furthermore reworked the text in terms of style and grammar to make the issues at hand clearer.

I am always struggling with the fact how inversions and carbon data assimilation handle the fact that the model must be spun up properly before it can be used. This issue is addressed somewhat in Section 5 but still needs more discussion. In particular, even after reading this manuscript, I am still unclear what value does a prior have when the parameter values have been suddenly changed. In a climate-mode a change in parameter values mean that the model must be spun up again to make its pools reach new equilibrium. As a result, don’t the optimized parameters in the MPI-CCDAS system also account for the fact that the model wasn’t spun up and brought to the present day using optimized parameters. Also, as soon as the new optimized parameters are used (without the model being spun up properly) doesn’t it mean that if the model were to run long enough it will eventually start drifting towards its "true" equilibrium.

In principle we agree here with the reviewer in that the parameter estimates we obtain are somewhat influenced by the choice of the spin-up method. The challenge with the carbon cycle is that the global carbon cycle is not in equilibrium and it is difficult to assess how far it departs from the equilibrium state (e.g. because of lack of historical information on land-use change etc. pp). Simply spinning up the model into equilibrium with the new parameters will therefore not be sufficient, because one will additionally have to run the model in a transient phase with the driving forces (CO2, climate, land-use etc.), which cause the current imbalance. At the current state, this is, albeit desirable, computationally not feasible. An alternative to a correct spin-up procedure, is to have accurate initial carbon pools. Hence we decided (also for runtime consideration – a spin-up is computationally expensive) to allow the MPI-CCDAS to also change the initial carbon pools directly. The relative simple approach adopted with only one global modifier was motivated by the long runtime of the framework (a few months). The results and discussion then reveal that the framework needs to be improved on that aspect. We also agree that the system will drift towards the „true“ equilibrium which is – rather then a deficit – a behaviour of any transient system. Whether the models equilibrium is in accordance with the „true“ equilibrium can only be reasonably assessed with long time series and potentially with repeated applications of systems like an MPI-CCDAS.

We already have this sentence in the text, which to our understanding describes the point very

clearly:
„In addition, we accounted for non steady-state conditions of the net carbon flux by estimating a global scaling factor for the size of the initial slow pool“

I have several handwritten comments in the attached supplement (an annotated ver- sion of manuscript) which indicates the places where sentences and words were un- clear.
See the comments below

The choice of colors in Figures 3 and 7 is really bad which doesn't allow a reader to evaluate results.
Without being more specific here, it is difficult for us to guess where the problems with the colours arise from. Maybe the reviewer was surprised by the fact that the difference maps do not show very large differences (with exceptions, but those have been discussed in the text). Since the other two reviewers did not mention this problem, we leave the figures as they are, unless we get more specific comments on how to improve the colours.

Finally, had the manuscript been in a single column mode with double spaced lines it would have been an easier read.
So far as I know I have no control over the layout that GMD produces with the input files. Sorry for this.

The reply to the handwritten comments follow here:
P1L10:
Computationally efficient refers to runtime, which is a limiting factor in global carbon cycle assimilations. We added a statement to the introduction to clarify this.

P1L16-17:
Assimilation of two data streams does not guarantee to fit both data streams equally well. There could be conflicting model formulations that avoid a good fit to all data streams.

P2L62:
Corrected

P2L63-67:
These processes are the simulated phenology, and its seasonal and interannual climate sensitvity, as well as the simulated seasonal net land-atmosphere carbon flux. We added these details to the text.

P2L91:
Corrected throughout the manuscript (following the GMD-standard)

P2L97:
p_po are the posterior parameters. We clarified this.

P3L1ff:
We apologize for the missing text. The missing text was:
„Technically, J is minimized through an iterative procedure using the Davidon-Fletcher-Powell algorithm in the Broyden-Fletcher-Goldfarb-Shanno variant in the implementation provided by the Numerical Recipes (Press et al., 1992, dfpmin routine). The required gradient $\partial J/\partial p$ is evaluated by the tangent-linear model ….“
It will be added to the revised manuscript

P3L58:

This is the naturally occurring heterogeneity within the area covered by one grid-cell (e.g.: due to different forest species but also variability within one species). We reformulated this to make the point clearer.

P3L76:
We added more details to the text (also for the temperature memory) and also refer to Knorr et al. (2010) for even more details.

P4L44:
Corrected throughout the manuscript

P5L17:
This has been corrected.

P5L50:
This has been corrected.

P6 Table 2:
The column headings have been clarified.

P7L4-5:
In changing the heterotrophic respiration, the net carbon flux to/from the atmosphere is also changed. As a consequence the atmospheric carbon content and its changes (the growth rate) is also modified. We try to make this clearer.

P7L35:
The term „wider“ is misleading in the text. We didn't intend to say that the set of cross-evaluation stations is larger then the set of stations used for assimilation. We changed the text accordingly.

P7L51ff:
These ancillary flux-fields are prescribed and we give here basically a short reference from where we have taken these field. These fields were not altered during the assimilation. We clarified this in the text

P7 Figure 1:
Yes the colour bar indicates the FAPAR uncertainty (between 0 and 1) and yes the uncertainty of FAPAR estimate is large. We added some clarification to the figure caption to make clear that the colour bar refers to FAPAR.

P8L13:
This has been added.

P8L26:
We mean here the soil carbon pool. This has been clarified

P8L23-36:
No, the model will not approach the prior state, because we changed the model parameters and they will remain at their posterior value also when no constraints are active. We clarified this in the text.

P8L57-58:
Necessary iterations were tens to hundreds and the total runtime was 1-2 months. We clarified this in the text

P8L66/68/70:
This has been corrected

P8L85:
We mean the norm of the gradient of the cost-function with respect to parameters. This has been clarified in the text

P8L87:
Iterations of the assimilation procedure. This has been clarified

P9L13:
Yes this is globally averaged. We clarify this in the text

P9L37:
We meant deciduous needle leaved. We have corrected this in the text.

P9L52:
We assimilate FAPAR observations to optimize model parameters. These are then used to run the model and to simulate FAPAR. So even though the observed and modelled FAPAR should be fairly similar after assimilation, there are still differences (e.g. because of observational or model uncertainties).

P10 Figure2:
The point is the mean and the vertical lines the uncertainties given with the 1*sigma uncertainty. We clarified this.

P12L2-7:
This refers to the period of 2005 – 2009. We clarified this in the caption of table 6.

P12-14:
Yes in all experiments (see table 6). We clarified this in the text.

P13 Figure 5:
We do not show a model vs. observation plot because in the current plot we can give also the information on the latitudinal gradient of the seasonal cycle amplitude (which would be hard to give in a simple model vs. observation plot). Since the behaviour of the latitudinal gradient in the assimilation is a relevant information, we keep this plot, even though it might be more difficult to read then a model vs. observation plot.

P13L3-6:
We directly control the size of the initial soil carbon pool by the modifier f_slow. We clarify this in the text.

P14 Figure 8:
The figure shows the value of posterior minus prior divided by the prior uncertainty. We clarify this in the figure caption.

P14L66-69:
We mean that the difference does not largely influence the models capability to reproduce the high-latitude season cycle of atmospheric CO2. This has been clarified.

P15L48 - 49:
This is a 3-D data set and also contains temporal information. This is clearly stated in the description of the observational operator representing the atmospheric transport.

P15L80:
We added the suggestion to the text.

P16L75:
We in fact mean what we write. It is not only atmospheric CO2 but it is rather the carbon cycle as represented in JSBACH (e.g. carbon stocks). We clarify this in the text.

P16L86:
The statement is not limited to atmospheric CO2 but is also valid for other observations of the global carbon cycle. Hence we leave this as it is.

P17L40:
With stiffness we mean here, that there are only few degrees of freedom to control the respiration in the MPI-CCDAS. We clarify this in the text.

P17L62-75:
In order to shorten the manuscript we removed this part because the important points are covered elsewhere in the manuscript

P18L11:
We mean, that the current network of CO2 observations only helps constraining the net carbon flux of relatively large regions. Finer resolved features (e.g. on the scale of European countries) are not well constrained.

Constraining a land surface model with multiple observations by application of the MPI-Carbon Cycle Data Assimilation System

G. J. Schürmann[a], T. Kaminski[b,d], C. Köstler[a], N. Carvalhais[a], M. Voßbeck[b,d], J. Kattge[a], R. Giering[c], C. Rödenbeck[a], M. Heimann[a], and S. Zaehle[a]

[a]Max Planck Institute for Biogeochemistry, Hans-Knöll-Str. 10, 07745, Jena, Germany
[b]The Inversion Lab, Hamburg
[c]FastOpt, Hamburg
[d]previously at FastOpt, Hamburg

Correspondence to: G. Schürmann(gschuer@bgc-jena.mpg.de) and S. Zaehle (soenke.zaehle@bgc-jena.mpg.de)

Abstract. We describe the Max Planck Institute Carbon Cycle Data Assimilation System (MPI-CCDAS) built around the tangent-linear version of the land surface scheme of the MPI-Earth System Model v1 (JSBACH). The simulated terrestrial biosphere processes (phenology and carbon balance) were constrained by observations of the fraction of absorbed photosynthetically active radiation (TIP-FAPAR product) and by observations of atmospheric CO_2 at a global set of monitoring stations for the years 2005 - 2009. When constrained by TIP-FAPAR alone, the system successfully, and computationally efficiently, improved simulated growing season average FAPAR, as well as its seasonality in the Northern extra-tropics. When constrained by atmospheric CO_2 observations, global net and gross carbon fluxes were improved, although the system tended to underestimate tropical productivity. Assimilating both data streams jointly allowed the MPI-CCDAS to match both observations (TIP-FAPAR and atmospheric CO_2) equally well as the single data stream assimilation cases, therefore overall increasing the appropriateness of the resultant biosphere dynamics and underlying parameter values. Our study thus demonstrates the value of multiple-data stream assimilation for the simulation of terrestrial biosphere dynamics. and highlights the potential role of remote sensing data, here the TIP-FAPAR product in stabilising the strongly underdetermined atmospheric inversion problem posed by atmospheric transport and CO_2 observations alone. The constraint on regional gross and net CO_2 flux patterns is limited through the parametrisation of the biosphere model. We expect improvement on that aspect through a refined initialisation strategy and inclusion of further biosphere observations as constraints.

1 Introduction

Estimates of the net carbon balance of the terrestrial biosphere are highly uncertain, because the net balance cannot be directly observed at large spatial scales (Le Quéré et al., 2015). Studies aiming to quantify the contemporary global carbon cycle therefore either infer the terrestrial carbon budget as a residual of the arguably better constrained other components of the global carbon budget (Le Quéré et al., 2015), or rely on measurements of atmospheric CO_2 and the inversion of its atmospheric transport (Gurney et al., 2002). Both approaches have the caveat that they are not able to provide accurate estimates at high spatial resolution, and cannot utilise the broader set of Earth system observations that provide information on terrestrial carbon cycle dynamics (Luo et al., 2012). Further, they are diagnostic by nature, and therefore lack any prognostic capacity.

Ecosystem models integrate existing knowledge of the underlying processes governing the net terrestrial carbon balance and have such a prognostic capacity. Since they simulate all major aspects of the terrestrial carbon cycle, they can - in principle - benefit from the broader set of Earth system observations. However, studies comparing different land surface models show a large spread of estimates of the seasonal and annual net land-atmosphere carbon exchange and their trends (Piao et al., 2013; Sitch et al., 2015). This uncertainty is one of the primary causes for discrepancies in future projections of stand-alone terrestrial biosphere models (Sitch et al., 2008), and coupled carbon cycle climate model projec-

tions (Anav et al., 2013; Friedlingstein et al., 2014) for the 21st century. Next to the uncertainty due to different climate forcing (Jung et al., 2007; Dalmonech et al., 2015) and alternative model formulations (Sitch et al., 2015), the uncertainty about the parameter values of the mathematical representation of key carbon cycle processes in these models are an important source of the model spread (Knorr and Heimann, 2001; Zaehle et al., 2005; Booth et al., 2012). This parametric uncertainty can be as large as the differences between models. The spread among models limits our ability to provide further constraints of the net terrestrial carbon uptake.

A potential route to reduce parameter and process-formulation related uncertainties in the estimates of the terrestrial carbon cycle is to systematically integrate the increasing wealth of globally distributed carbon cycle observations into models through data assimilation methods. A broad overview of potential observations and methodological choices is given in Raupach et al. (2005). Knorr and Kattge (2005) investigated the use of a Monte-Carlo approach for data assimilation with global models and suggested that the computational burden (run time) is too large to allow its use with a comprehensive land surface model and a reasonable number of parameters in the optimisation. Notwithstanding this constraint, for a reduced set of parameters Ziehn et al. (2012) managed to successfully apply a Monte Carlo algorithm to the BETHY model in global set-up, albeit with limited process representations. Since computational run time is still a limiting factor in global carbon cycle data assimilation, the development of a relatively "fast" system is advantageous over other assimilation methods. A computationally more efficient method is to to use gradient-based methods. For instance, approximating the gradient with finite differences,Saito et al. (2014) performed assimilation of several data streams with the VISIT model. An alternative to finite difference is to calculate the gradient precisely by a tangent-linear or adjoint version of the biosphere model. A prototype of such a carbon cycle data assimilation system (CCDAS) based on an advanced variational data assimilation scheme and a prognostic terrestrial carbon flux model (BETHY; Knorr 1997, 2000) has demonstrated the potential to effectively constrain the simulated carbon cycle with observations of atmospheric CO_2 (Rayner et al., 2005; Scholze et al., 2007; Kaminski et al., 2013). Conceptually similar systems have been built for other global biosphere models. For example, Luke (2011) constrained the phenology of the JULES model with the MODIS collection 5 leaf area index product and Kuppel et al. (2012, 2013) applied the ORCHIDEE model at a series of FLUXNET-sites to estimate process parameters across these sites and further demonstrated the usefulness of the approach to improve globally modelled CO_2. Bacour et al. (2015) assimilate different FAPAR observations with the ORCHIDEE model (in-situ and satellite) at selected sites and report a large influence on the results depending on the FAPAR-product. Forkel et al. (2014) assimilated FAPAR into the model LPJmL to assess long term control on vegetation greenness. Kaminski et al. (2012) assimilated FAPAR jointly with CO_2 as a constraint and Kato et al. (2013) assimilated the net carbon fluxes and FAPAR jointly at a FLUXNET site.

~~Removed the old paragraph reviewing the CCDAS-Systems which is now replaced by the one above~~

Here we present the development and first application of the variational data assimilation system built around the JSBACH (Raddatz et al., 2007) model (Max Planck Institute Carbon Cycle Data Assimilation System: MPI-CCDAS), based on the tangent-linear representation of JSBACH. JSBACH is a further development of the BETHY model, providing a more detailed treatment of carbon turnover and storage in the terrestrial biosphere, as well as more detailed treatment of land surface biophysics (Roeckner et al., 2003) and land hydrology (Hagemann and Stacke, 2014), and the land surface scheme of the MPI-Earth System Model (MPI-ESM; Giorgetta et al., 2013).

Our objective with this development is twofold: i) to improve the scope of the original BETHY-CCDAS (see: Kaminski et al., 2013) by including a larger set of terrestrial processes affecting the terrestrial carbon cycle; and ii) to provide a means to constrain the land carbon cycle projections of JSBACH with several data streams, and in hindsight also that of the MPI-ESM. Dalmonech et al. (2015) have shown that the simulated phenolgy, and its seasonal and interannual climate sensitvity, as well as the simulated seasonal net land-atmosphere carbon flux are reasonably robust against climate biases in the MPI-ESM. One can therefore expect that improvements of these aspects made with the MPI-CCDAS driven by observed meteorology will be maintained in the coupled Earth system model. Further, at the example of assimilating atmospheric CO_2 and TIP-FAPAR, we demonstrate the mutual benefit of the two data streams in constraining parameters in JSBACH.

~~While the MPI-CCDAS is driven with observed meteorology, and differences in the simulated terrestrial carbon cycle between JSBACH with observed meteorology or coupled to the ESM exist (Dalmonech et al., 2015), certain features of the land processes are robust to the climate biases of the MPI-ESM, such that one might expect an improved carbon representation in the entire MPI-ESM after application of the MPI-CCDAS.~~

We first provide a technical description of the MPI-CCDAS system. We then demonstrate the capacity of the MPI-CCDAS system to simultaneously integrate atmospheric CO_2 observations and the fraction of absorbed photosynthetically active radiation (FAPAR) recorded from satellites, which constrains the seasonality of the phenology, and assesses the relative effect of the constraint from these two data streams on parameter values and modelled fluxes.

2 Description of MPI-CCDAS

2.1 CCDAS-Method

The MPI-CCDAS relies on a variational data assimilation approach to estimate a set of model parameters. In the following we give a brief overview of this method, and refer for a detailed description to Kaminski et al. (2013). To take account of the uncertainty inherent in the description of observed and simulated variables the method operates on probability density functions (PDFs). It is conveniently formulated in a Gaussian framework and uses the combined information provided by the model $M(\boldsymbol{p})$ and the observations $\boldsymbol{d}$ to update a PDF that describes the prior state of information on the parameter vector $\boldsymbol{p}$ (more precisely on the control vector, which is a combination the model's process parameters and of initial state variables). This prior control vector is described by the mean $\boldsymbol{p}_{pr}$ and the covariance of its uncertainty $\mathbf{C}_{pr}$. The CCDAS method seeks to minimize the missfit between observed and modelled quantities by minimizing the cost function J

$$J(\boldsymbol{p}) = \frac{1}{2}\left(M(\boldsymbol{p})-\boldsymbol{d}\right)^T \mathbf{C}_d^{-1}\left(M(\boldsymbol{p})-\boldsymbol{d}\right) + \left(\boldsymbol{p}-\boldsymbol{p}_{pr}\right)^T \mathbf{C}_{pr}^{-1}\left(\boldsymbol{p}-\boldsymbol{p}_{pr}\right) \quad (1)$$

where $\mathbf{C}_d$ is the covariance of combined uncertainty in the observations (with mean $\boldsymbol{d}$) and model simulation. The minimum ~~$\boldsymbol{p}_{\overline{po}}$~~ of J , denoted as $\boldsymbol{p}_{po}$ (the posterior control vector), is the maximum likelihood estimate. $\boldsymbol{p}_{po}$ thus balances the misfit between modelled quantities and their observational counterparts over the entire assimilation window, while taking independent prior information on the control vector into account. This means the vector d contains all observations, which act to simulatenously constrain the control vector. In contrast to sequential assimilation schemes, this approach determines a model trajectory through the state space, which, in particular, ensures convervation of mass and energy (see, e.g., Kaminski and Mathieu, 2016).

Technically, J is minimized by a quasi Newton approach with so-called Broyden-Fletcher-Goldfarb-Shanno (BFGS) updates of the Hessian approximation, ~~through an iterative procedure using the Davidon-Fletcher-Powell algorithm in the Broyden-Fletcher-Goldfarb-Shanno variant~~ in the implementation provided by the Numerical Recipes (Press et al., 1992, dfpmin routine). The iterative procedure requires the gradient ~~required gradient~~ $\frac{\partial J}{\partial p}$, which is evaluated by the tangent-linear version of the model that was generated by TAF (Giering and Kaminski, 1998) via automatic differentiation (AD: Griewank 1989) of the model's source code. The fundamental modes of AD, forward and reverse, respectively produce tangent-linear and adjoint codes, by application of the chain rule. Unlike the traditional approximation by finite or divided differences of model runs (numerical differentiation), tangent-linear and adjoint codes provide derivative information that is accurate up to machine precision.

The values and uncertainties for the control and observational vectors as well as the model are detailed in the following sub-sections.

2.2 The forward model

The model that is optimised within the MPI-CCDAS is the land surface model JSBACH (Raddatz et al., 2007; Brovkin et al., 2009; Reick et al., 2013; Schneck et al., 2013; Dalmonech and Zaehle, 2013). The model considers ten plant functional types (PFTs: see Table 1). These PFTs are allowed to co-occur within one grid cell on different tiles, but nonetheless share a common water storage. Compared to the aforementioned JSBACH studies, the MPI-CCDAS does not use land-use change and land-use transition nor dynamic vegetation, but uses a multi-layer soil hydrology scheme (Hagemann and Stacke, 2014). JSBACH is typically used within the MPI-ESM (Giorgetta et al., 2013) and calculates the terrestrial storage of energy, water and carbon and its half-hourly exchanges between the atmosphere and the land surface. JSBACH is applied here uncoupled from the atmosphere and forced with reconstructed meteorology (see Sec. 3).

The application of gradient-based minimisation procedures is facilitated by a differentiable ~~implementation~~ calculation of $J(\boldsymbol{p})$. According the the chain rule, this ultimately requires all code parts of the forward model that depend on the control variables and impact the cost-function to be differentiable. To improve differentiability, the original phenology scheme, which describes the timing and amount of foliar area based on logistic growth functions (Lasslop, 2011) was replaced by the alternative scheme developed explicitly for this purpose (Knorr et al., 2010) (see Sec. A). Some further minor modifications were necessary to make the code differentiable. These changes included replacing look-up tables with their continuous formulations, avoiding division by zero in the derivative code (e.g. through ~~evaluation~~ differentiation of $\sqrt{0}$ in the forward mode leading to $\frac{1}{\sqrt{0}}$ in the diffentiated code) , and reformulating minimum and maximum calculations to allow a smooth transition at the edge. These modifications alter the calculations, however, they were implemented such that the differences in the modelled results compared to the original code is minimal.

~~Sections 2.2.1 to 2.2.4 have been moved to the appendix~~

2.2.1 Atmospheric transport

To map the net land-atmosphere CO_2 exchange simulated by JSBACH to observations of the atmospheric CO_2-mole fraction, the computation of atmospheric transport is required, which is done here by the transport model TM3 (Heimann and Körner, 2003). Specifically, we compute the response of monthly mean CO_2 mole fractions $\boldsymbol{c}$ to monthly mean sur-

Table 1. Plant functional types that are optimised and the limitations that control the phenological behaviour of the respective functional type.

Plant functional type	Limitations
Tropical evergreen trees (TrBE) Tropical deciduous (TrBS) Raingreen shrubs (RS)	Water
Coniferous evergreen trees (CE) Extra-tropical deciduous trees (ETD) Coniferous deciduous (CD)	Temperature and Daylight
C3-grasses (TeH) C3-crops (TeCr) C4-grasses (TrH) C4-crops (TrCr)	Temperature and Water

face fluxes $\boldsymbol{f}$ (extending 2 years back in time). Since the atmospheric transport is linear (in the fluxes), this can be written as:

$$\Delta \boldsymbol{c} = \mathbf{M} \cdot \boldsymbol{f} \tag{2}$$

where $\mathbf{M}$ represents the TM3 responses as a transport matrix. In the MPI-CCDAS these ~~and multiply these~~ transport matrices (or Jacobians) are multiplied with the net CO_2 exchange as in Rödenbeck et al. (2003). The net exchange is the sum of the terrestrial fluxes computed by JSBACH and those not computed by JSBACH, i.e. ~~and~~ prescribed ocean and fossil fuel fluxes. Biomass burning fluxes are not explicitly included (see also discussion in Sect. 5.6) and these fluxes are consequently mapped to the respiratory part of JSBACH during the assimilation of atmospheric CO_2 The mole fraction at the beginning of this simulation is specified as a globally constant offset CO_2^{offset}, one of the parameters to be estimated. The resulting CO_2-mole fractions can then be directly compared with observed atmospheric CO_2. Limiting the system to one global modifier was motivated by limitation in the computational run time, while an inclusion of an offset depending on the observation locations could be easily implemented. With a spin-up of 2 years for the atmospheric transport, we allow the system to build up the latitudinal gradient of CO_2. After the second year, there is no visible trend in the difference of observed CO_2 at Mauna Loa and South Pole. Thus 2 years are sufficient to spin-up the atmosphere.

For our analysis, we used the Jacobian representation of the TM3 model, version 3.7.24 (Rödenbeck et al., 2003), with a spatial resolution of about 4°x5° (the "fine" grid of TM3 by Heimann and Körner 2003), driven by interannually varying wind fields of the NCEP reanalysis (Kalnay et al., 1996).

2.3 Model parameters

For this study, JSBACH parameters related to the phenology, photosynthesis and land carbon turnover (including initial carbon stocks) are ~~estimated~~ optimized (see appendix A for a more detailed description on the relevant parts of JSBACH). The default prior value and assumed prior Gaussian uncertainty ~~(with Gaussian distribution)~~ of each parameter and the ~~, as well as~~ posterior values from the assimilation experiments are given in Table 2. The choice of these parameters was based on an extensive parameter sensitivity study on a much larger set of parameters across multiple biomes (Schürmann, unpublished results). We retained those parameters, for which we found a significant effect on modelled FAPAR and net CO_2 exchange. In principle, it is possible to add more parameters, which are decisive for other modelled quantities such as soil moisture and which might feed back to our observables. A brief explanation of the parameters involved in this study is given in the following.

The parameters controlling the phenology (Λ_{max}, τ_l, τ_w, T_ϕ, t_c, and ξ) are allowed to take different values for different plant functional types with the exception of ξ, which is valid globally. While Λ_{max} controls the maximum amount of leaves, ξ controls the rate of leaf growth, and τ_l is the time-scale of leaf senescence. T_ϕ and t_c are temperature and day-length tresholds, respectively, controlling the onset and end of vegetation activity. The parameter τ_w controls the shedding of leaves in response of phenology for drought-deciduous PFTs. Soil moisture in JSBACH follows a 5-layer scheme (Hagemann and Stacke, 2014) and is coupled to the vegetation via the phenology and the photosynthesis by influencing actual stomatal conductance. ~~Their~~ The phenological parameter prior values and uncertainties are taken from Knorr et al. (2010), with the following three exceptions: the water control parameter τ_w required an adaptation to account for the different soil-water formulations in the MPI-ESM compared to BETHY, τ_l for the coniferous evergreen (CE) PFT also has been adapted after preliminary site-scale studies to allow more flexibility in the seasonality of the evergreen-phenology (Schürmann, unpublished results) and, finally, Λ_{max} is left to its default JSBACH parameter value for all PFT's with the exception of the coniferous evergreen (CE) PFT. For this PFT a value of $\Lambda_{max} = 1.7\,\mathrm{m}^2/\mathrm{m}^2$ has been used, because preliminary model tests revealed a large bias in modelled FAPAR in CE-dominated regions, which adversely affected the model results of the carbon cycle. ~~(see also Sect. 5.5).~~

Photosynthesis in JSBACH follows Farquhar et al. (1980) for C3-plants and Collatz et al. (1992) for C4- plants, with details as described in Knorr and Heimann (2001) and Knorr (1997). To estimate gross assimilation directly, maximum carboxylation rate Vc_{max} and maximum electron transport J_{max} are allowed to vary per PFT. We assume that the observed tight correlation between Vc_{max} and J_{max} is conserved irrespective of the precise value for each PFT (Kattge

Table 2. Parameters that are part of the control vector with their prior and posterior values of the global assimilation experiments. Parameters marked with a * are multiplied with their respective value in the model, given in Table D1. The mapping variants are explained in the appendix C: 1: No lower bound; 2: A lower bound at 0 for those parameters that are not allowed to take negative values.

Representation in Eq. 1:		$\mathbf{C}_{pr}$	$\boldsymbol{p}_{pr}$	$\boldsymbol{p}_{po}$				
Parameter(PFT)	**Description**	**Prior sigma**	**Prior**	**JOINT**	**CO2alone**	**FAPARalone**	**Unit**	**Mapping**
Λ_{max} (TrBE)*	Maximum LAI	0.2	1	0.98	0.82	0.84	.	2
Λ_{max} (TrBD)*	Maximum LAI	0.2	1	0.58	0.55	0.63	.	2
Λ_{max} (ETD)*	Maximum LAI	0.2	1	0.98	1.04	1.44	.	2
Λ_{max} (CE)*	Maximum LAI	0.2	1	1.00	0.84	1.01	.	2
Λ_{max} (CD)*	Maximum LAI	0.2	1	0.64	1.31	0.56	.	2
Λ_{max} (RS)*	Maximum LAI	0.2	1	1.33	0.94	1.24	.	2
Λ_{max} (TeH,TeCr)*	Maximum LAI	0.1	1	0.63	0.53	0.61	.	2
Λ_{max} (TrH,TrCr)*	Maximum LAI	0.1	1	0.53	0.49	0.59	.	2
$1/\tau_l$ (ETD)	Leaf shedding time scale	0.01	0.07	0.057	0.057	0.079	d^{-1}	2
$1/\tau_l$ (CE)	Leaf shedding time scale	1e-04	5e-04	0.00067	0.00045	0.00064	d^{-1}	2
$1/\tau_l$ (CD)	Leaf shedding time scale	0.01	0.07	0.068	0.07	0.068	d^{-1}	2
$1/\tau_l$ (TeH,TeCr)	Leaf shedding time scale	0.01	0.07	0.098	0.076	0.079	d^{-1}	2
$1/\tau_l$ (TrH,TrCr)	Leaf shedding time scale	0.01	0.07	0.077	0.07	0.07	d^{-1}	2
τ_w (TrBE)	Water stress tolerance time	30	300	319.82	378.04	286.77	days	2
τ_w (TrBD)	Water stress tolerance time	10	114	107.78	120.84	106.29	days	2
τ_w (RS)	Water stress tolerance time	5	50	49.51	50.02	47.82	days	2
τ_w (TeH,TeCr)	Water stress tolerance time	25	250	222.32	215.22	230.41	days	2
τ_w (TrH,TrCr)	Water stress tolerance time	25	250	276.06	236.32	286.64	days	2
T_ϕ (ETD)	Temperature at leaf onset	1	9.21	7.19	8.63	2.28	°C	1
T_ϕ (CE)	Temperature at leaf onset	1	9.21	7.53	9.01	7.61	°C	1
T_ϕ (CD)	Temperature at leaf onset	1	9.21	0.10	5.53	0.30	°C	1
T_ϕ (TeH,TeCr)	Temperature at leaf onset	0.5	1.92	3.82	2.67	2.78	°C	1
T_ϕ (TrH,TrCr)	Temperature at leaf onset	0.5	1.92	2.50	1.57	1.88	°C	1
t_c (ETD)	Day length at leaf shedding	1	13.37	13.57	13.84	13.60	hours	2
t_c (CE)	Day length at leaf shedding	1	13.37	14.22	13.69	14.12	hours	2
t_c (CD)	Day length at leaf shedding	1	13.37	14.94	13.66	14.73	hours	2
ξ	Initial leaf growth rate	0.03	0.37	0.41	0.38	0.43	d^{-1}	2
f_{photos} (TrBE)*	Photosynthesis rate modifier	0.1	1	0.75	1.02	0.91	.	2
f_{photos} (TrBD)*	Photosynthesis rate modifier	0.1	1	1.07	1.08	0.97	.	2
f_{photos} (ETD)*	Photosynthesis rate modifier	0.02	1	0.99	1.00	1.00	.	2
f_{photos} (CE)*	Photosynthesis rate modifier	0.03	1	0.95	1.00	1.00	.	2
f_{photos} (CD)*	Photosynthesis rate modifier	0.06	1	1.04	1.05	1.00	.	2
f_{photos} (RS)*	Photosynthesis rate modifier	0.1	1	1.01	1.05	1.00	.	2
f_{photos} (TeH)*	Photosynthesis rate modifier	0.1	1	0.96	1.01	0.99	.	2
f_{photos} (TeCr)*	Photosynthesis rate modifier	0.1	1	0.67	0.86	1.00	.	2
f_{photos} (TrH)*	Photosynthesis rate modifier	0.1	1	1.04	1.02	1.06	.	2
f_{photos} (TrCr)*	Photosynthesis rate modifier	0.1	1	0.87	0.94	1.00	.	2
Q_{10}	Temperature sensitivity of resp.	0.15	1.8	1.90	1.81	1.80	.	2
f_{slow}	Multiplier for initial slow pool	0.1	1	0.50	0.51	1.00	.	2
f_{aut_leaf}	Leaf fract. of maintenance resp.	0.1	0.4	0.30	0.35	0.40	.	2
CO_2^{offset}	Initial atmospheric carbon	3	0	0.90	0.85	0.00	ppm	1

and Knorr, 2007). Thus, we introduce a single scaling coefficient f_{photos}:

$$Vc_{max} = Vc_{max}^{prior} \cdot f_{photos} \quad (3)$$

$$J_{max} = J_{max}^{prior} \cdot f_{photos} \quad (4)$$

Prior parameter ranges for each PFT were derived from the TRY data-base (Kattge et al., 2011).

Autotrophic respiration in JSBACH follows Knorr (2000) where growth respiration is a fixed fraction (20 %) of the net assimilation. Maintenance respiration scales with dark respiration (with a parameter f_{aut_leaf}) assuming to be coordinated with foliar photosynthetic activity. Net primary production is allocated to either a green or woody pool which turns to three litter pools (above ground green, below ground green and woody) with distinct PFT-specific turnover times. Heterotrophic respiration of these pools responds to temperature according to a $Q10$ formulation (see appendix A). The prior sensitivity studies revealed that the most influential parameters controlling Carbon storage on land and partitioning between autotrophic and heterotrophic respiration were the leaf fraction of maintenance respiration (f_{aut_leaf}) and temperature response (Q_{10}) of the carbon pools, which were both included as parameters into the optimisation. The uncertainty of these parameters was based on expert knowledge, and inspired by the works of Mahecha et al. (2010) for $Q10$ and Knorr (2000) for f_{aut_leaf}.

To account for non steady-state conditions of the net carbon flux, we followed the approach of Carvalhais et al. (2008) by estimating a global scaling factor for the size of the initial slow pool f_{slow}. The inclusion of f_{slow} to the optimized parameters ~~This~~ allows for the modification of global heterotrophic respiration and hence also an adjustment of the CO_2 growth rate via altering the net carbon flux from or to the atmosphere. ~~, but~~However, the limitation is that this does not change the spatial distribution of carbon pools, which remains controlled by the prior parameter values. For this first application of the MPI-CCDAS, the most slowly varying pool has been selected (i.e. the soil carbon pool with a turnover time of 100 years). The initial conditions of other carbon pools were not included in the control vector to avoid the associated increase in the computational burden (e.g. run time). This consequently includes the risk of assigning any misrepresentation of modelled pools sizes to the soil carbon pool and the changes in the carbon pool sizes after the assimilation should be interpreted with care. The uncertainty of f_{slow} has been set to 10 %, reflecting a moderate deviation from equilibrium (but see also discussion in Sect. 5.5). The turnover-time parameters (see Eq. A18) were not included in the assimilation experiment, because their impact on land carbon fluxes was small compared to other parameters (Schürmann, unpublished results) at the time-scale of the MPI-CCDAS (a couple of years).

To account for minor offsets of the MPI-CCDAS with respect to the initial carbon content of the atmosphere, one single offset value CO_2^{offset} is included in the set of estimated parameters. CO_2^{offset} was assumed to not deviate more than a few ppm, and its uncertainty set accordingly.

Uncertainties on all parameters were assumed to be Gaussian and exposed to the assimilation procedure in a form normalized by their prior uncertainty. In order to prevent parameters from attaining physically impossible, negative values, some parameters were constrained at the lower end of the distribution to zero (see Table 2 and appendix C).

2.4 Observational constraints and observation operators

2.4.1 Atmospheric CO_2

Observed atmospheric CO_2 mole fractions were obtained from the flask data/continuous measurements provided by different institutions (e.g. flask data of NOAA/CMDL's sampling network, update of Conway et al. 1994, Japan Meteorological Agency - JMA, Meteorological Service of Canada - MSC, and many others; see Rödenbeck et al. 2003). Stations were selected in order to cover the global latitudinal gradient (Table B1), focussing on remote locations with little imprint of local fluxes. For cross-evaluation, ~~a wider~~a disjunct set of available station data were used (Table B2). The temporal resolution of the CO_2 original data at the monitoring stations (hourly to daily/weekly) depends on the specific station and were averaged into monthly means.

~~For our analysis, we used the Jacobian representation of the TM3 model, version 3.7.24 (Rödenbeck et al. 2003), with a spatial resolution of about 4 °x5° (the "fine" grid of TM3 by Heimann and Körne 2003), driven by interannually varying wind fields of the NCEP reanalysis (Kalnay et al. 1996).~~ The MPI-CCDAS compares atmospheric CO_2 at a monthly temporal resolution, considering the sampling of simulated CO_2 abundance at the same time in which measurements were available in order to reduce the representation error. The treatment of the observations of CO_2 and their uncertainties are done as in Rödenbeck et al. (2003). A floor value of 1 ppm is added to this uncertainty, similarly as in Rayner et al. (2005). Ancillary flux fields at monthly resolution were prescribed ~~used~~ to represent the ocean (Jena CarboScope pCO2-based mixed layer scheme oc_v1.0 Rödenbeck et al., 2013) and fossil fuel (Emissions Database for Global Atmospheric Research EDGAR, European Commission, Joint Research Centre (JRC)/Netherlands Environmental Assessment Agency (PBL) 2009) net CO_2 fluxes.

2.4.2 TIP-FAPAR

The observations of FAPAR that have been assimilated were specifically derived for this study by the Joint Research Centre Two-stream Inversion Package (JRC-TIP, Pinty et al.

2007). The product was derived by running JRC-TIP on MODIS broadband visible and near-infrared white sky surface albedo input aggregated to the model grid separately for snow-free and snow-like background conditions in a similar way as described for the native 0.01 degree product (Pinty et al., 2011a, b; Clerici et al., 2010; Voßbeck et al., 2010). ~~Uncertainties in the FAPAR data are based on rigorous uncertainty propagation using first and second derivative information (Voßbeck et al. 2010).~~ JRC-TIP has been explicitly designed to deliver products suitable for assimilation into climate and numerical weather prediction models. It is based on an advanced one dimensional two-stream scheme Pinty et al. (2006) that assures a physically consistent solution of the radiative transfer problem in the coupled canopy-soil system. Similar schemes are implemented in most state-of-the-art terrestrial biosphere models (see, e.g. Loew et al., 2014). Uncertainties in the FAPAR data are based on rigorous uncertainty propagation from the MODIS input albedos using first and second derivative information (Voßbeck et al., 2010). A space and time invariant prior (except for the occurrence of snow) is used, i.e. all spatio-temporal variability in the products is derived from the input products (including the MODIS snow flag). In contrast to alternative algorithms there is no variability imposed through (possibly implicit) assumptions, e.g. on land cover (as in Knyazikhin et al., 1999), which avoids inconsistencies, e.g. with the model's own land cover (for more details see Disney et al. (2016)). To reduce biases in the retrieved products through the prior information, the prior is given a deliberately low weight, e.g. a sigma of 5 for the effective LAI (Pinty et al., 2011a).

We applied two filters on the global FAPAR product to assure that potential model structural errors did not lead to compensating effects in the parameter estimation procedure and thus impede fitting the FAPAR data in other regions. First, owing to the fact that no specific crop-phenology is implemented in JSBACH, grid cells with fractional crop coverage of more than 20 % have been filtered out, as we cannot expect the model to fit cropland phenology. A consequence of this filter is to mask the deciduous broadleaf PFT in the US and Europe, because in these areas, this PFT is collocated in crop-dominated pixels. Hence, the phenological parameters of the deciduous broadleaf PFT are only constrained by observations from other locations - a fact that should be kept in mind when interpreting the deciduous broadleaf parameters. Second, grid-points with correlations between the prior model and the observed FAPAR below 0.2 (i.e. prior phenology exhibits out-of-phase seasonal cycles) have also been filtered out. Together, these filters reduce the overall global coverage of the FAPAR-constraint and thus the number of observations to be fitted (Fig. 1) by 57 %.

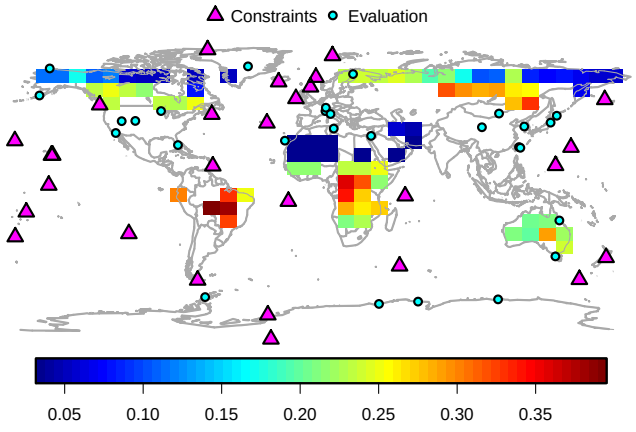

Figure 1. Location of the CO_2 observations (for constraining the model and for evaluation) and the median over the time series of the TIP-FAPAR uncertainties (given with the color-scale) in each pixel acting as constraint

3 Experimental set-up

The MPI-CCDAS is driven by daily meteorological forcing (air temperature, specific humidity, precipitation, downward short- and longwave radiation, wind speed) obtained from the WATCH forcing data set (Weedon et al., 2014). Annual CO_2 mole fractions of the atmosphere as a forcing for the photosynthesis calculations of JSBACH were prescribed according to Sitch et al. (2015). Vegetation distribution (Fig. E1) and other surface characteristics are derived from Pongratz et al. (2008). Although the MPI-CCDAS is flexible to be run at any spatial resolution, for computational efficiency, we have set-up the MPI-CCDAS at a coarse spatial resolution of about 8°x10°, even though the atmospheric transport itself was simulated at 4°x5°, because the precomputed Jacobians have been calculated at that resolution.

For the water and carbon cycle state-variables of JSBACH, the following spin up procedure was applied: First, an equilibrium was achieved through an integration over the period 1979-1989 with corresponding meteorological forcing and atmospheric CO_2 mole fractions of 1979. Starting from this equilibrium state, a transient integration from 1979 to 2003 followed. The final state of 2003 was then taken as the initial condition for all MPI-CCDAS experiments. This spin-up procedure used the prior parameter values, i.e. it was not part of the assimilation loop for the parameter estimation. To allow a direct control of the non-equilibrium states of the carbon pools, the initial soil carbon ~~slow~~ pool (at the end of the spin-up procedure) was multiplied by a global scaling factor that is part of the parameter estimation procedure (see Sect. 2.3).

The MPI-CCDAS itself was run for the years 2003 - 2011, i.e. parameters were left free to adapt to the observational constraints. The first two years (2003 to 2004) allowed the system to build a spatial gradient in the simulated atmo-

spheric CO_2 mole fractions. In the following years (2005 to ~~and~~ 2009) the observational constraints were active. For the consecutive two years (2010 to 2011), the constraints were inactive and the observations were used to evaluate the MPI-CCDAS with posterior parameters in hindcast-model.

As evaluation statistics, we used the correlation, bias, root mean squared error and the Nash-Sutcliffe model efficiency (NSE). The latter is defined as:

$$NSE = 1 - \frac{\sum_i (d_i - m_i)^2}{\sum_i \left(d_i - \overline{d_i}\right)^2} \quad (5)$$

where the index i denotes individual pairs of observation (d) and model output (m) and an overbar the arithmetic mean. $NSE = 1$ indicates a perfect model and for all $NSE < 0$ the mean of the observations is a better predictor than the model itself.

Our study follows a factorial design to assess the benefit of each data stream, but also to evaluate the potential of assimilating more than one data stream and its effect on the carbon cycle. Therefore, we conducted three experiments: two experiment assimilating each one data stream alone (CO2alone using only CO_2 and FAPARalone using only TIP-FAPAR) and one experiment assimilating both data streams simultaneously (JOINT), with each data stream equally weighted in the cost function (Eq. 1).

4 Results

4.1 Performance of the assimilation

The application of the MPI-CCDAS to the given problem (FAPARalone, CO2alone, or JOINT) was successful within an appropriate number (tens to hundreds) of iterations (with run-times of 1 - 2 months), increasing from FAPARalone (using only TIP-FAPAR), to CO2alone (using only CO_2), and JOINT (using both observations simultaneously as a constraint; Table 3): For all three assimilation experiments, the value of the cost-function was considerably reduced, while the posterior parameter values remained in physically plausible ranges, even though a few (e.g.: T_ϕ of the coniferous deciduous phenotype) deviate strongly from the prior values (Table 2). For FAPARalone, the value of the cost function was almost halved between prior and posterior run. Even stronger reductions of the cost function were obtained in the other two experiments using also CO_2 (Table 3). ~~Interestingly, the posterior cost of the JOINT assimilation roughly equals the sum of the single data-stream experiments, indicating consistency of the model with both data streams.~~ Several statistics comparing the posterior model with observations for FAPAR and CO_2 (Tables 4 and 5) show that the model performance of the JOINT experiment was comparable to the performance of the two single data-stream experiments relative to the assimilated quantity. While the JOINT assimilation captured the main features of both data sources, the single data-stream assimilation experiments either showed no improvement with respect to the other data stream (such as the CO2alone case for FAPAR), or even a degradation (such as the FAPARalone case for CO_2). Overall, these results suggest that both data streams can be successfully assimilated jointly with the MPI-CCDAS.

During the assimilation procedure, the norm of the gradient[1] $\frac{\partial J}{\partial p}$ (see Eq. 1) was considerably reduced by 3 - 4 orders of magnitude (Table 3). The behaviour was such that during the first tens of iterations of the assimilation procedure, the cost as well as the norm of the gradient were considerably reduced. Also the parameter values changed the most in this initial phase of the assimilation. However, they also changed in later iterations without substantial reductions in the cost function or the norm of the gradient. The assimilation then finally stopped, because the changes to the parameters became too small. ~~Notably, the norm did not approach zero for the cases using CO_2 as a constraint, as would have been expected for the minimum of the cost-function. This is an indication that for these experiments our posterior parameter estimate does not yet minimize the cost function: a point also mentioned by Rayner et al. (2005) with respect to their CO_2 assimilation with the BETHY-CCDAS.~~ In the following we discuss the performance of the assimilation with respect to FAPAR and CO_2 in detail.

4.2 Phenology

The statistics of the comparison with the TIP-FAPAR data sets shows an improvement of the model-data fit for all experiments relative to the prior model (Table 4), which as expected is strongest when using FAPAR (FAPARalone and JOINT) as a constraint.

One important reason for the improvement was a general reduction in modelled growing-season average FAPAR simulated by the MPI-CCDAS compared to the prior run. This decrease in FAPAR was mostly driven by a reduction of globally averaged foliar area of 0.41 m^2m^{-2} ~~on average~~ for the JOINT experiment (0.34 m^2m^{-2} for FAPARalone and 0.59 m^2m^{-2} for CO2alone). Almost all PFTs contributed to the decrease in FAPAR following a reduction in the maximum leaf area index parameter (Λ_{max}) for tropical deciduous forests, needle-leaf deciduous forests, as well as herbaceous PFTs (crops and grasses). The water-stress parameter τ_w played a secondary role in the leaf area reduction by affecting the maximum leaf-area for drought responsive PFTs (see Table 1). The concurrent increase of foliar area for extra-tropical deciduous and rain green shrubs only plays a minor role in the model-data agreement, since these PFTs only cover a small fraction of the global land area.

In regions with a strong temperature control of phenology, the assimilation did not only change the ~~magnitude~~ average LAI ~~of the phenological seasonal cycle~~ during the

[1] The norm of a vector $\boldsymbol{v}$ is: $\|\boldsymbol{v}\| = \sqrt{\boldsymbol{v} \cdot \boldsymbol{v}}$

Table 3. Characteristics of the assimilation experiments. The prior and posterior cost-function values and the contribution of FAPAR, CO_2 and the prior (second term in Eq. 1) to the posterior cost-function value are given as well as the norm of the gradient and the number of observations acting as a constraint and the number of iterations of the assimilation

Experiment name	Prior cost	Posterior cost	FAPAR cost	CO_2 cost	Parameter cost	Prior norm of the gradient	Posterior norm of the gradient	Number of observations	Number of iterations
CO2alone	1922	344	0	287	57	12196	14.8	1524	69
FAPARalone	1431	723	626	0	97	208	0.7	3189	29
JOINT	3352	1102	682	309	112	12162	6.1	4713	69

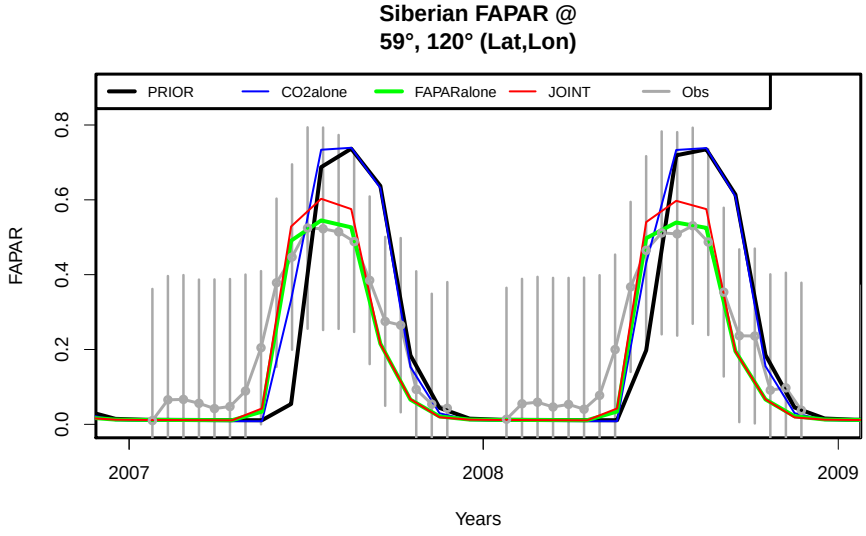

Figure 2. Example time-series of FAPAR for an East Siberian pixel dominated by the CD-PFT to demonstrate the improvement in the timing of the phenology after the assimilation. TIP-FAPAR observations are given with their mean (dots) and $1 \cdot \sigma$ uncertainties (vertical lines). ~~$1 \cdot \sigma$ uncertainties~~

growing season. As demonstrated by the enhanced correlation and model efficiency of the MPI-CCDAS with respect to the TIP-FAPAR data (Table 4), also the timing of onset and end of the growing season was improved. This improvement was mostly the result of adjusting the parameters T_ϕ and t_c, which are temperature and day-length criteria that determine when the vegetation switches from the dormant to the active phase. In particular, the assimilation reduced the temperature control parameter T_ϕ, which led to an earlier onset of the growing season in the extra-tropical deciduous broadleaf and deciduous needleleaf PFTs. For the deciduous ~~evergreen~~needleleaf forests the assimilation procedure also resulted in an earlier end of the growing season, in accordance with the observations (see Fig. 2 for an example). ~~For the other PFTs, these parameters changed not as pronounced, leading to no notable difference in the phenological timing - at least not at the analysed monthly temporal resolution.~~ The parameters controlling the phenological timing of other PFTs were not strongly altered by the assimilation, which - at the monthly temporal resolution of the satellite data analysed here - led to no observable modification of the temporal behaviour of FAPAR. Notably, also the CO2alone experiment showed some improvement in the correlation and model efficiency compared to TIP-FAPAR, although this experiment did not use the TIP-FAPAR data as a constraint. This suggests that the seasonal cycle of CO_2 bears some constraint on the timing of ~~N~~northern extra-tropical phenology.

While the FAPARalone assimilation run performs best compared with TIP-FAPAR (Table 4), the FAPARalone and JOINT assimilation runs are fairly similar (though not identical) with respect to the simulated FAPAR. The temporally averaged LAI (Fig. 3) demonstrates the overall similarity between the FAPARalone and JOINT experiments. This similarity is also reflected in the parameter values of the phenology: the parameters of FAPARalone and JOINT often were closer to each other than to CO2alone (Table 2). - An example for this are the tropical evergreen tree PFTs, for which parameters of the JOINT and FAPARalone experiment are different while the modelled foliar area is very similar. A further explanation for this feature highlighting the importance of multi-data stream assimilation is given in Sec. 4.4.1. The most pronounced differences between the JOINT and FA-

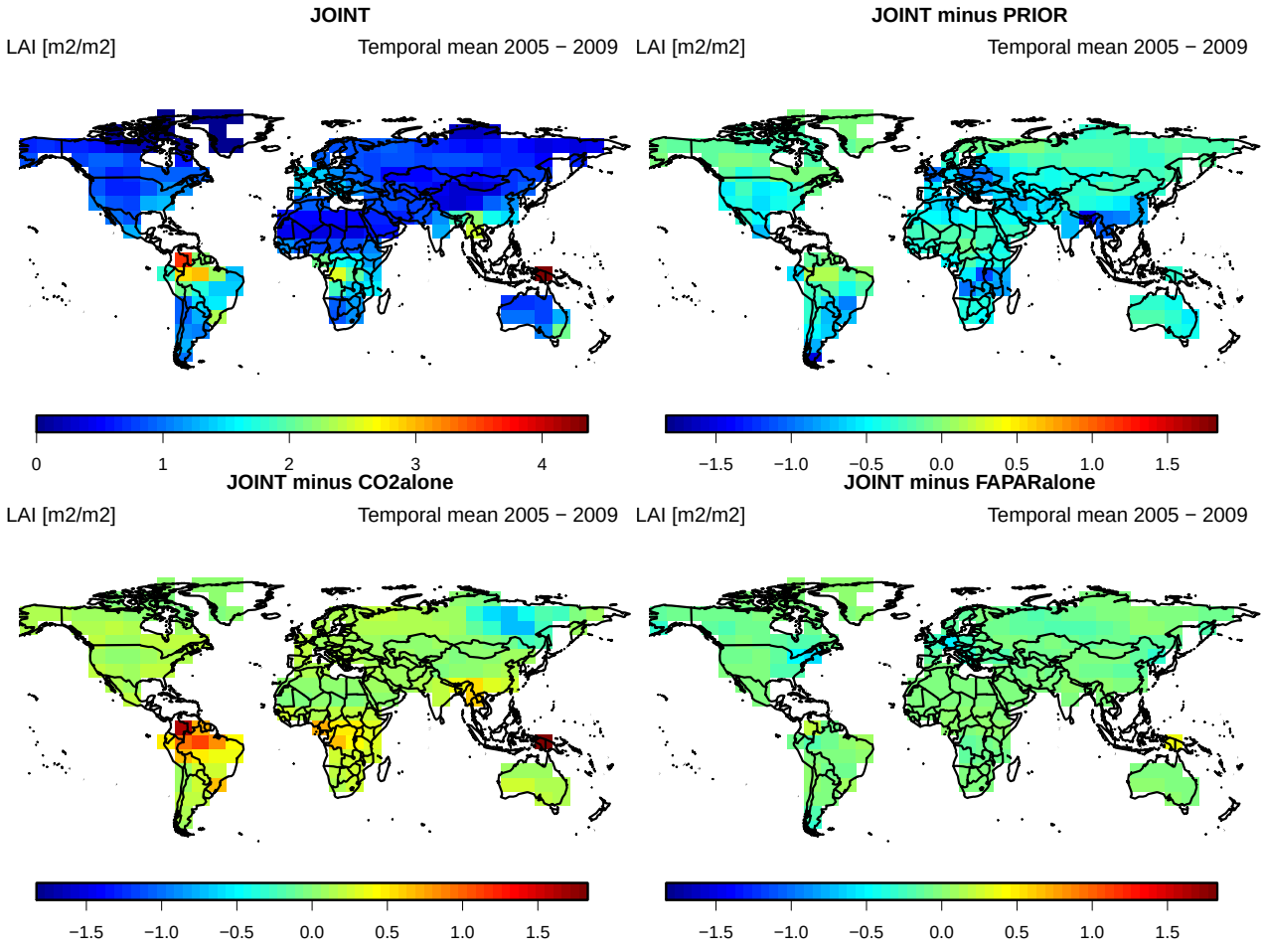

Figure 3. Temporally averaged global LAI of the JOINT experiment and differences of the other experiments to the JOINT case.

Table 4. Performance of the prior and posterior models compared with TIP-FAPAR observations (applying the same data quality screening as for the assimilation). The assimilation period (2005 - 2009) as well as a subsequent evaluation period (2010/2011) is shown. Abbreviations are: Bias: Model - Observations, Corr: Correlation, RMSE: Root mean squared error, NSE: Nash Sutcliffe model efficiency.

	2005 - 2009				2010/2011			
	Corr	Bias	RMSE	NSE	Corr	Bias	RMSE	NSE
PRIOR	0.60	0.069	0.19	0.10	0.61	0.075	0.19	0.12
CO2alone	0.66	-0.072	0.17	0.31	0.67	-0.074	0.17	0.31
FAPARalone	0.72	-0.014	0.14	0.51	0.73	-0.013	0.14	0.52
JOINT	0.71	-0.022	0.14	0.49	0.72	-0.022	0.14	0.50

PARalone experiment, leading also to the differences in the globally averaged foliar area, arose at locations where TIP-FAPAR data were not used as constraints in e.g. crop dominated pixels (where also the extra-tropical deciduous tree (ETD) PFT covered a substantial part of the grid-cell).

Larger differences in FAPAR were obtained with the CO2alone and JOINT experiments (Table 4 and Fig. 3). The CO2alone experiment showed the smallest LAI, and thus the smallest FAPAR. This feature is especially pronounced in tropical regions, where the decrease is driven by the water-control parameter τ_w and the maximum foliar area Λ_{max}. This pattern is countered by larger foliar area than the JOINT experiment for coniferous deciduous trees, driven by the parameter Λ_{max} which is increased for CO2alone, but decreased for the other two experiments. A likely explanation of this behaviour is given in Sect. 4.4.2.

4.3 Atmospheric CO_2

The assimilation procedure strongly reduced the misfit between observed and modelled atmospheric mole fraction of CO_2 when using CO_2 as a constraint (Table 5). This was true for the seasonal cycle, the seasonal cycle's amplitude and the 5-years trend (Fig. 4 and 5). Conversely, the FAPARalone experiment showed a strong deterioration of the simulated atmospheric CO_2 metrics compared to the prior model. Notwithstanding an improvement of the seasonal cycle amplitude of atmospheric CO_2 (Fig. 5), the 5-years trend of atmospheric CO_2 was much less conforming to the observations, leading to a much faster increase in CO_2 than observed (Table 5 and Fig. 4). Notably, introducing TIP-FAPAR as an additional constraint in the JOINT experiment did allow the MPI-CCDAS to match both the atmospheric CO_2 data and the TIP-FAPAR product: the simulated monthly CO_2 mole fractions of the JOINT and CO2alone experiment are almost identical for most sites (Table 5 and Fig. 4 and 5).

The improvement of the simulated atmospheric CO_2 for the CO2alone and JOINT assimilation run persisted for the two years following the assimilation period, in which the model was run in a hindcast mode (driven by reconstructed meteorology), with only minor degradation in model performance (Table 5). Both experiments clearly outperform the prior model, which is most obvious in the improvement of the Nash-Sutcliffe model efficiency for the hindcast period.

The comparison of the simulated posterior atmospheric CO_2 mole fractions at the evaluation stations showed a general improvement in the performance measures, with substantial improvements in the simulated bias, RMSE and Nash-Sutcliffe model efficiency relative to the prior model (Table 5). Unlike for the set of calibration sites, there was no difference in the improvement between the assimilation period and the subsequent two-year period, suggesting that the model improvement is of general nature. In other words, the short-term (1-2 years) prognostic capabilities of the model have been largely improved for a 2 years horizon after assimilating CO_2-observations, also at the evaluation locations.

4.3.1 Changes in Carbon fluxes causing the changes in simulated CO_2

The changes in simulated atmospheric CO_2 mole fractions originate from substantial changes of the seasonal amplitude and overall strength of the net carbon fluxes simulated by of JSBACH. The application of the CO_2-constraint increased the global net biome production (NBP) from 1.0 $PgCyr^{-1}$ in the prior model to 3.2 $PgCyr^{-1}$ in the CO2alone and JOINT experiments. Conversely, using only TIP-FAPAR as a constrained decreased the NBP to -2.2 $PgCyr^{-1}$, in other words, turning the biosphere into a net source (Table 6), inconsistent with current understanding of the global carbon cycle (Le Quéré et al., 2015). Despite the similarity of the global NBP for the experiments with CO_2 as a constraint, the spatial patterns of the NBP are different between the CO2alone and JOINT experiments (Fig. 6). The net uptake in both experiments originates from boreal and tropical regions. However, while the JOINT experiment shows an uptake in the boreal regions of coniferous evergreen and coniferous deciduous dominated pixels, the net CO_2 uptake in the CO2alone experiment is more concentrated to the coniferous deciduous regions. These differences will be further discussed in Sect. 4.4.2.

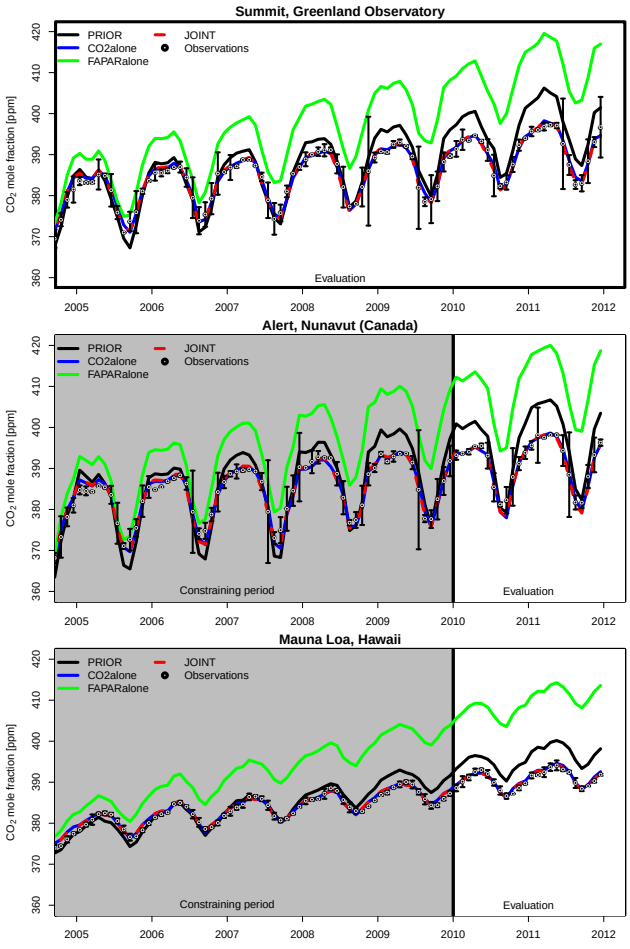

Figure 4. Time series of CO_2 as observed at the high latitude evaluation site Summit and at two constraining sites, one at high latitudes (Alert) and one representative for the Northern Hemisphere (Mauna Loa) for the different prior and posterior models. The observations are given together with their uncertainty.

While the atmospheric observations constrain the net land-atmosphere CO_2 flux, the MPI-CCDAS model parameters affect the gross-fluxes, and thus the changes in NBP are again the consequence of substantially altered gross fluxes and land carbon pools. The generally reduced foliar area directly leads to a reduced gross primary production (GPP) of the terrestrial biosphere (in all experiments). The changes to the photosynthetic capacity (f_{photos}) (Table 2) often further reduce the uptake, a factor which is most pronounced for crop and tropical

Table 5. Performance of the prior and posterior models compared with atmospheric CO_2 for constraining and evaluation sites and for the assimilation period (2005 - 2009) and the hindcast period (2010/2011). Abbreviations are: Bias: Model - Observations, Corr: Correlation, RMSE: Root mean squared error, NSE: Nash Sutcliffe model efficiency.

	2005 - 2009				2010/2011			
	Corr	Bias	RMSE	NSE	Corr	Bias	RMSE	NSE
Stations acting as constraint								
PRIOR	0.95	0.64	2.60	0.68	0.93	4.85	5.22	-0.69
CO2alone	0.96	-0.05	1.32	0.92	0.93	0.10	1.47	0.87
FAPARalone	0.91	8.91	9.84	-3.63	0.91	18.21	18.35	-19.86
JOINT	0.96	-0.09	1.35	0.91	0.93	-0.16	1.48	0.87
Stations withheld from assimilation								
PRIOR	0.86	1.20	3.83	0.52	0.84	5.18	6.03	-0.61
CO2alone	0.89	0.25	2.54	0.79	0.89	0.19	2.19	0.79
FAPARalone	0.84	9.73	10.84	-2.87	0.86	18.89	19.12	-15.14
JOINT	0.88	0.24	2.61	0.78	0.88	-0.05	2.28	0.77

Table 6. Global averages of selected carbon cycle components for the years 2005 to 2009 in $\mathrm{PgC\,yr^{-1}}$ for fluxes and PgC for stocks and comparison with other estimates. Ra: autotrophic respiration. Rh: heterotrophic respiration. Reco: ecosystem respiration. Vegetation carbon is made up of all carbon stored in the living parts of the vegetation (including above and belowground carbon of plants and woods.)

	PRIOR	CO2alone	FAPARalone	JOINT	Other estimates	Other CCDAS
NPP	65.5	40.9	53.5	45.6	$44-66^a$	40^g
Ra	86.1	57.6	67.8	65.7		
Rh	64.5	37.6	55.4	42.2		
Reco	150.6	95.2	123.2	107.9		
GPP	151.6	98.4	121.3	111.3	$119\pm6^b, 123\pm8^c$	$109-164^h$
NBP	1	3.2	-2.2	3.2	2.4 ± 0.8^d	
Soil Carbon	2649	1064.7	2187.1	1122.3	1343^e	
Vegetation Carbon	424	388.5	420.5	407.3	442 ± 146^f	
Litter Carbon	239.9	189.8	212.8	193.9		

[a]Cramer et al. (1999); Saugier and Roy (2001); [b]Jung et al. (2011); [c]Beer et al. (2010); [d]Le Quéré et al. (2015); [e]http://webarchive.iiasa.ac.at/Research/LUC/External-World-soil-database/HTML/; [f]Carvalhais et al. (2014); [g]Rayner et al. (2005); [h]Koffi et al. (2012)

evergreen PFTs (Table 6 and Table 2). The GPP reduction is strongest for the CO2alone experiment and weakest (but still very pronounced) for FAPARalone. Even though the globally integrated posterior GPP values were somewhat different, the relative latitudinal patterns were fairly similar to each other (Fig. 7), and the reduction occurred in all regions, predominantly in tropical forests and grass/crop dominated temperate and boreal zones (Table 2).

Since the net carbon fluxes in the FAPARalone experiment were not constrained by the atmospheric CO_2 observations, the assimilation did not adjust the ecosystem respiration to balance the reduced productivity induced from the altered FAPAR. In the JSBACH model, autotrophic respiration is estimated as a direct function of GPP and canopy integrated carboylation capacity (Eq. A17), and thus quickly adjusts to any changes in GPP, On the time scales of five years in this study, this decline was not sufficient to balance the reduced GPP. As a consequence, the net flux to the atmosphere increased leading to the overestimation of the growth rate of atmospheric CO_2. Application of the CO_2 constraint in the CO2alone and JOINT experiment forces ecosystem respiration to be further reduced to match the atmospheric signal. This additional reduction in ecosystem respiration is mainly driven by a reduction of the initial soil carbon pool (via the modifier f_{slow}) to 50% and 51% for the JOINT and CO2alone experiment, respectively, which reduces heterotrophic respiration (Table 6 ; see also discussion in Section 5.5).

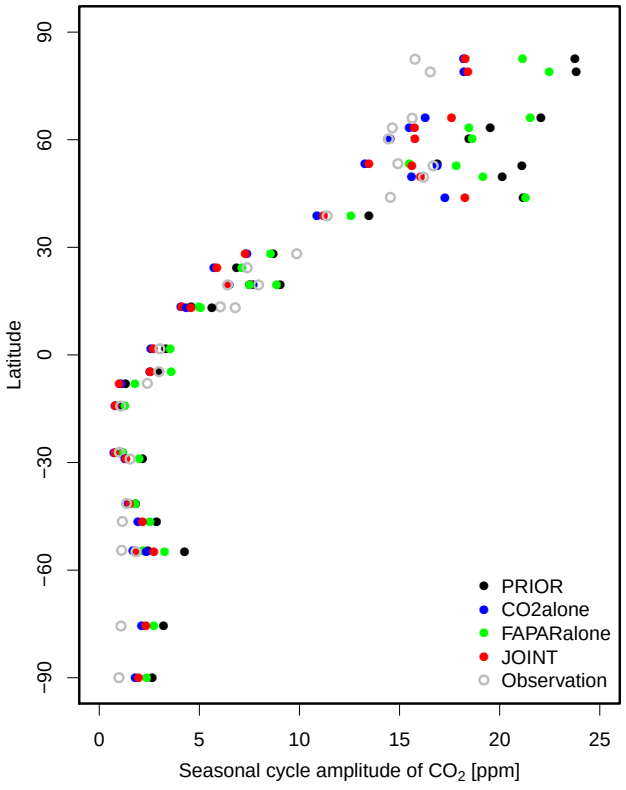

Figure 5. Latitudinal distribution of atmospheric CO_2 seasonal cycle amplitude, calculated as the difference between the maximum and minimum CO_2 mole fraction of the averaged seasonal cycle of the linearly de-trended signal from 2005 - 2009.

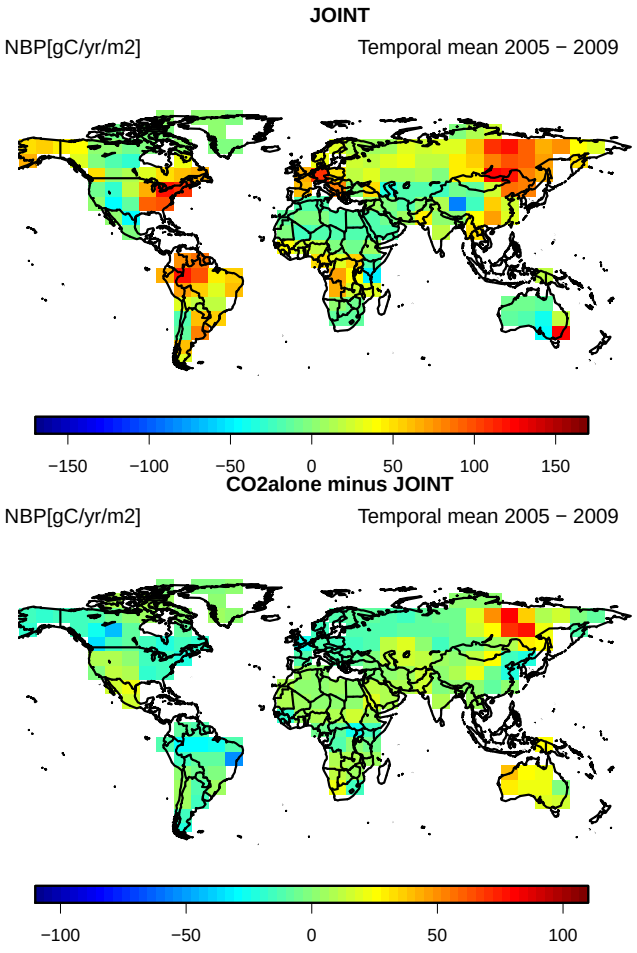

Figure 6. Temporally averaged NBP of the JOINT assimilation, differences of CO2alone to the JOINT experiment and the latitudinal distribution for the prior and posterior models.

4.4 Regional differences among the experiments

In the following, we focus on differences in the spatial patterns of the results obtained for tropical regions and the boreal zone to highlight the interplay between parameters in a global, multi-data stream application of the MPI-CCDAS either by compensating effects between different model processes within one PFT as occurring in the tropics (Sect. 4.4.1) or by compensations between different parts of the globe (Sect. 4.4.2).

4.4.1 Tropics

The modelled foliar area in the tropics (mainly the tropical evergreen tree PFT) was similar for the JOINT and FAPARalone experiments (Fig. 3), but smaller for CO2alone. The simulated GPP of the JOINT experiment (Fig. 7) was somewhat lower than in the FAPARalone experiment, but still substantially larger than that of the CO2alone experiment. Notwithstanding these differences, the simulated net land-atmosphere CO_2 exchange (Fig. 6) of the JOINT experiment was closer to the posterior estimate of CO2alone than to that of FAPARalone in terms of absolute values.This result was caused by compensating effects of the different observational constraints (Fig. 8 and Table 2): the phenological parameters, notably τ_w and Λ_{max}, were substantially different between the FAPARalone and JOINT exper-

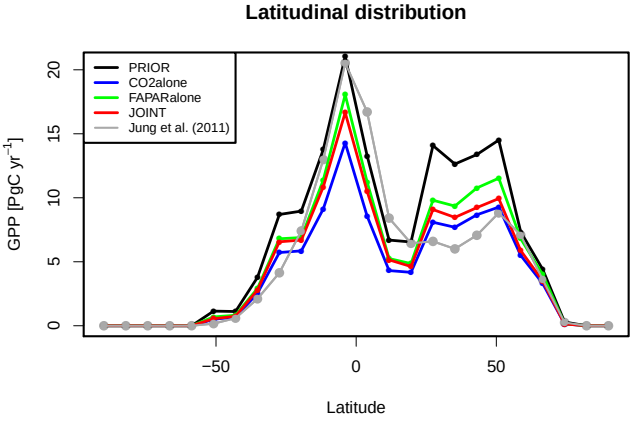

Figure 7. Latitudinal distribution of GPP for the prior and posterior models and comparison with the estimates of Jung et al. (2011).

iment, yet their modelled foliar area was very similar (Fig. 3). The reason for this was that the photosynthesis parameter modifier f_{photos} was reduced strongly in the JOINT experiment, which also drives the smaller GPP (relative to FAPARalone). ~~A consequence of this large reduction in modelled photosynthesis per unit foliar area and ecosystem level GPP was a strong decrease in the potential transpiration rate (E_{pot}; Eq. A5) through the effect of net photosynthesis on canopy conductance (Eq. A14).~~ Through the effect of net photosynthesis on canopy conductance (Eq. A14), the potential transpiration rate (E_{pot}; Eq. A5) was strongly decreased. Together with the increase of τ_w (Eq. A5) in the JOINT experiment, the decline in E_{pot} had the same effect on the simulated phenology as the smaller parameter changes in the FAPARalone experiment. The lack of an FAPAR constraint in the CO2alone experiment allowed the assimilation to overly reduce the foliar area by increasing τ_w at the prior rate of photosynthesis and thus E_{pot} to satisfy the constraint by the atmospheric CO_2 observations. As a consequence, due to the water-cycle feedback, the modelled foliar area was clearly different between the JOINT and CO2alone experiments.

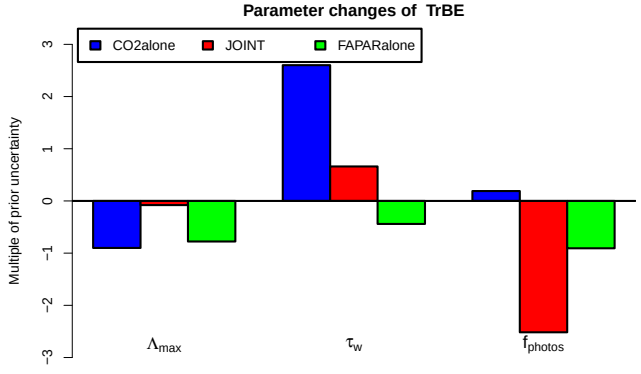

Figure 8. Parameter changes of tropical evergreen trees in multiples of the prior uncertainty (as $\frac{p_{po}-p_{pr}}{\sigma_{pr}}$).

4.4.2 Boreal zones

The CO2alone and JOINT experiments showed similar global statistics when compared with atmospheric CO_2 observations (Table 5 and Fig. 4). Their global and hemispheric net carbon uptake was similar (Northern Hemisphere: 2.24/2.20 $\mathrm{PgC\,yr^{-1}}$; Southern Hemisphere: 0.98/0.98$\mathrm{PgC\,yr^{-1}}$), but their underlying spatial patterns were different, in particular in the boreal zone (Fig. 6). The entire boreal zone took up a large share of the global carbon sequestration in the JOINT experiment (0.88 $\mathrm{PgC\,yr^{-1}}$), especially in coniferous deciduous (CD) dominated regions of Eastern Siberia (0.30 $\mathrm{PgC\,yr^{-1}}$). The CO2alone experiment showed a similar net Carbon uptake in the boreal region, but the uptake in the CD dominated region was 0.16 $\mathrm{PgC\,yr^{-1}}$ stronger than in the JOINT experiment. This difference was mainly driven by larger foliar area and increased leaf-level productivity (parameter f_{photos}) of the CD PFT in the CO2alone experiment. In the same latitudinal band, coniferous evergreen trees showed reduced foliar area in the CO2alone experiment compared to the JOINT experiment, reducing the net uptake by 0.16 $\mathrm{PgC\,yr^{-1}}$, such that the differences in these regions cancel each other. These relatively small spatial differences ~~can nevertheless be seen as minor differences in the ability of the~~ do not prevent the posterior JOINT and CO2alone experiment ~~in~~ from capturing the amplitude of the seasonal cycle at individual northern-most stations.

This largely increased sink in Eastern Siberia could be an artefact of the set-up used for the data assimilation in this study. No nearby atmospheric stations constrains the net carbon sink in this region adequately, and the CD PFT only occurs dominantly in this region. In consequence, the PFT's parameters can not be adequately constrained by carbon cycle observations from other parts of the globe. This relative scarceness of observations and independency of other regions allows the East-Siberian net carbon uptake to compensate for other regions fluxes in order to match the global growth rate. Additional observations would be required to allow for spatially higher resolved estimation of the net fluxes.

5 Discussion

5.1 Comparison of the simulated Carbon cycle with independent estimates

We have demonstrated that the JSBACH model is capable of reproducing the seasonal cycle and five years trend of the observed atmospheric CO_2 (Fig.s 4 and 5 and Table 5). During the assimilation run, we have applied a careful selection of stations to avoid the impact of local sources on modelled atmospheric CO_2 mole fractions, which cannot be simulated with the current coarse resolution of the MPI-CCDAS. The evaluation at the cross-validation sites, which are located on land and thus closer to locally varying source patterns, also demonstrates a good skill of the posterior model for these sites. Overall, this does suggest that the improvement of the MPI-CCDAS's capability to capture the observed CO_2 dynamics at monthly to yearly time scales is reasonably robust. Our results further support earlier studies (Rayner et al., 1999; Kaminski et al., 1999; Peylin et al., 2013) that the observational network of atmospheric CO_2 only constrains a limited number of spatio-temporal flux patterns.

The application of the CCDAS led to significant changes of the modelled carbon cycle in JSBACH. The average global GPP of the JOINT experiment ~~(111 $\mathrm{PgC\,yr^{-1}}$)~~ was substantially reduced from the prior run ~~(152 $\mathrm{PgC\,yr^{-1}}$)~~ and was slightly lower than independent, data-driven estimates of 119 $\pm$ 6 $\mathrm{PgC\,yr^{-1}}$ (Jung et al., 2011) and 123 $\pm$ 8 $\mathrm{PgC\,yr^{-1}}$ (Beer et al., 2010), as well as estimates of com-

parable land surface models (ranging from 111 - to 151 $\mathrm{PgC\,yr^{-1}}$; Piao et al. 2013). Partly driven by the reduction of GPP, the net primary production (NPP) was also significantly reduced ~~(from 66 $\mathrm{PgC\,yr^{-1}}$ (prior))~~ to 46 $\mathrm{PgC\,yr^{-1}}$ in the JOINT experiment. While this is lower than the commonly accepted reference value of 60 $\mathrm{PgC\,yr^{-1}}$, it is still compatible with the range of available estimates for NPP of 44 - 66 $\mathrm{PgC\,yr^{-1}}$ (Cramer et al., 1999; Saugier and Roy, 2001). The latitudinal distribution of GPP in comparison to an empirical estimate based on satellite data and field measurements (Jung et al., 2011) shows that the global reduction of GPP ~~occurred across the globe, leading~~ leads to a better agreement of GPP in the ~~N~~northern extra-tropics between 30°N and 60°N, but to a lower GPP ~~a smaller simulated GPP~~ in the tropical rain forests (Fig. 7). The reduction of GPP in the ~~N~~northern extra-tropics is likely associated with the overestimation of the seasonal cycle of atmospheric CO_2 by the prior model, which was successfully reduced primarily by reducing ~~N~~northern extra-tropical productivity, in particular in temperate and boreal grasslands. Nevertheless, our study supports earlier findings that despite some constraint on northern extra-tropic production, the constraint of observed atmospheric CO_2 on global production is small (Koffi et al., 2012).

A detailed comparison on the simulated vegetation and soil carbon stocks of the prior model is beyond the scope of this paper, partly because the simplifications of the spin-up procedure entail biases in predicted vegetation carbon stocks, as transient land-use changes and forest management, affecting forest age structure are ignored. It is nevertheless instructive to provide context for the simulated vegetation and soil carbon stocks by comparing them to the global totals of independent estimates. The posterior experiments showed only little less carbon in vegetation (389 - 420 PgC (composed of quickly overturning leaf and fine root carbon, as well as a woody carbon pool).) than the prior model (424 PgC). All of these estimates are lower than the 556 PgC vegetation carbon based on updated Olson's major world ecosystem carbon stocks[2], but comparable to a more recent estimate of global vegetation carbon storage of 442 ± 146 PgC (Carvalhais et al., 2014). The posterior amount of soil carbon from the assimilation runs using atmospheric CO_2 as a constraint compare favourably (within the uncertainty) to the estimates of 1343 PgC based on the Harmonized World Soil Database (HWSD)[3]. This estimate is more appropriate for the presented comparison than the more recent and higher estimate of soil carbon by Carvalhais et al. (2014) of 1836 - 3257 PgC (95% confidence interval), as the latter includes estimates of permafrost carbon, which is not modelled with the current version of the MPI-CCDAS.

[2]http://cdiac.ornl.gov/epubs/ndp/ndp017/ndp017b.html

[3]http://webarchive.iiasa.ac.at/Research/LUC/External-World-soil-database/HTML/

~~The above changes in the carbon cycle led to significant differences in the simulated annual net land carbon fluxes between the assimilation experiments. The assimilation experiments using atmospheric CO_2 as a constraint considerably increased the net land carbon uptake from 1.0 PgC in the prior run to 3.2 PgC during 2005-2009. This increase primarily occurred by reducing ecosystem respiration more than reducing GPP.~~

Our estimate of the net land carbon sink using atmospheric CO_2 as a constraint is slightly larger than the residual land carbon sink estimate (without inclusion of land-use change fluxes) inferred from atmospheric measurements and auxiliary fluxes by Le Quéré et al. (2015), who derived a net uptake of 2.4 ± 0.8 $\mathrm{PgC\,yr^{-1}}$ for the period 2000 - 2009. Correcting this estimate for the pre-industrial lateral carbon fluxes from land to the ocean via rivers would increase the terrestrial net land C uptake seen by the atmosphere (and thus the MPI-CCDAS) to 2.85 $\mathrm{PgC\,yr^{-1}}$; see Le Quéré et al. 2015 and Jacobson et al. 2007). Due to the interannual variability of the land sink, the shorter time-period of our sink estimate may have contributed to the difference between the estimates. More likely, one driving factor of our slightly larger estimate of the land net carbon uptake is from the comparatively small net ocean carbon uptake of 1.1 $\mathrm{PgC\,yr^{-1}}$ (Rödenbeck et al., 2013), which we prescribed in our assimilation. This compares to the estimate of 2.4 ± 0.5 $\mathrm{PgC\,yr^{-1}}$ of Le Quéré et al. (2015). Bearing in mind that the atmospheric CO_2 observations more directly constrain the net land carbon fluxes at seasonal and annual scales than the gross fluxes or carbon pools, assuming a larger ocean net carbon flux would have reduced the land uptake. Explicitly accounting for DOC based carbon losses from land in the future will help to close the gap between the estimates, and thereby reduce the estimated land carbon storage inferred from the atmospheric data, and allow for the estimate of the MPI-CCDAS to be more compatible with the estimate of Le Quéré et al. (2015).

5.2 Comparison to previous studies

Our results are consistent with earlier studies, which showed that JSBACH overestimates the seasonal cycle amplitude of atmospheric CO_2 (Dalmonech and Zaehle, 2013). The posterior estimates of this amplitude was considerably reduced and hence improved in all three experiments (Fig. 5). This also holds for FAPARalone, for which the comparison with CO_2 is an independent evaluation. Note that the prior we reported here already relies on a corrected maximum leaf area index (Λ_{max}) of coniferous evergreen trees (see Sect. 3). For the run with the off-the-shelf configuration of JSBACH (results not shown), the high latitude mean seasonal cycle amplitude was clustered around 30 ppm, implying an overestimation of about 15 ppm. In the prior experiment, this overestimation was reduced to about 5 - 10 ppm, and further reduced in the FAPAR alone experiment (Fig. 5). In other words, boreal phenology considerably controls the seasonal

cycle of the high latitude atmospheric CO_2-signal and TIP-FAPAR can improve this aspect even though the CO_2 trend is deteriorated (Fig. 4). Adding CO_2 as a constraint further improves the fit to the seasonal cycle amplitude.

This conclusion is also supported by Kaminski et al. (2012), who constrained the BETHY-CCDAS jointly with atmospheric CO_2 data and a different FAPAR product (Gobron et al., 2007). They found an improved seasonal cycle amplitude of CO_2 for their joint assimilation with real data, which is in line with our findings. Through factorial uncertainty propagation with their assimilation scheme, Kaminski et al. (2012) also found that the inclusion of FAPAR yields only a moderate uncertainty reduction in the simulated carbon fluxes and mainly reduces the water flux uncertainties. Kaminski et al. (2012) therefore suggested that FAPAR only added little information to the modelled carbon cycle in addition to atmospheric CO_2. In contrast, we have shown here a considerable impact of TIP-FAPAR by altering the spatial net Carbon flux patterns between the JOINT and CO2alone experiments.

Our study also showed a considerable difference of GPP estimates that are not likewise reflected in the net carbon fluxes, as these are more directly constrained by CO_2. Also Koffi et al. (2012), using a variant of the BETHY-CCDAS (Rayner et al., 2005; Scholze et al., 2007), found large differences in their posterior GPP-estimates ranging from 109 - 164 $\mathrm{PgC\,yr^{-1}}$ when using different transport models, atmospheric station densities and prior uncertainties. As in our study, their relatively large GPP-ranges are not reflected in the net fluxes, as these are more directly constrained by the atmospheric CO_2 network. A striking difference to the results of Koffi et al. (2012) occurs in the tropics, where they overestimate GPP compared to data-driven estimates, whereas the MPI-CCDAS underestimates GPP. As will be discussed later (Sect. 5.5), our underestimation of tropical GPP is likely a compensating effect arising from the respiration part of the model that only can be modified globally. This is not the case for the BETHY-CCDAS, which allows for a spatially more explicit control on heterotrophic respiration. It appears thus likely that a larger posterior GPP in the MPI-CCDAS could be expected with a system allowing for more spatial freedom in the respiration part of the assimilation system, for instance by making f_{aut_leaf} and f_{slow} vary by plant functional type. Regardless of this difference, our work further supports earlier findings (Rayner et al., 2005; Scholze et al., 2007; Koffi et al., 2012) that despite some constraint on ~~N~~northern extra-tropical GPP, the global land GPP cannot be well constrained with atmospheric CO_2 alone. It appears thus vital that additional information is provided, especially in tropical regions, to further reduce uncertainty in the spatial distribution of the gross fluxes GPP and ecosystem respiration. This likely will propagate to an improved estimate of the net CO_2-fluxes as well.

~~Within the BETHY-CCDAS, Rayner et al. (2005) found a very pronounced decrease of NPP from 68 $\mathrm{PgC\,yr^{-1}}$ in the prior run to 40 $\mathrm{PgC\,yr^{-1}}$ in the posterior run. This decrease was driven by a decrease of their parameter $f_{R,leaf}$ (a value also achieved by Scholze et al. 2007), which is functionally comparable to the MPI-CCDAS parameter f_{aut_leaf}. Their estimate is thus similar to our strong NPP-reduction (JOINT NPP: 46 $\mathrm{PgC\,yr^{-1}}$). This apparent similarity towards relatively small numbers (compared to other estimates) should not mislead to the conclusion that global NPP is well constrained from atmospheric CO_2, because it ignores spatial offsets between the estimates, and the fact that the MPI-CCDAS and BETHY-CCDAS approaches to estimate NPP from GPP are fairly similar. Assimilation of CO_2 into other, simpler biosphere models achieved ranges for NPP from 36 to 53 $\mathrm{PgC\,yr^{-1}}$ given different model formulations (Kaminski et al. 2002).~~

5.3 ~~Critical appraisal of the current MPI-CCDAS~~

~~With the set-up of the cost function and given the tangent-linear version of the JSBACH model, the assimilation problem for the MPI-CCDAS is clearly defined and solutions of the problem are by construction compatible with the model dynamics. This is a considerable difference to alternative methods, but also means that in the posterior estimates, any model structural deficits will be compensated for by unrealistic parameter values or can be detected in large model-data residuals. This allows to detect model structural errors and/or deficits in the set-up, which then can lead to a reformulation of the forward model (see e.g.: Kaminski et al., 2003; Rayner et al., 2005; Williams et al., 2009; Kaminski et al., 2013). The MPI-CCDAS framework described here can be steadily improved through regular improvements of the JSBACH model structure by including missing or correcting false model parametrisations (e.g. Knauer et al., 2015). The system is versatile enough to add more constraints from relevant and complementary, multiple data sources (Luo et al., 2012) to come up with more robust regional estimates than the current atmospheric inversion allow.~~

5.4 Discussion of the assimilation procedure

The results clearly show that two data-streams can be successfully integrated with the MPI-CCDAS. The posterior parameter values (Table 2) were different between the FAPARalone and JOINT, as well as the CO2alone and JOINT experiments, showing that the joint use of the two data streams added information to the posterior parameter vector by preventing the degradation of the phenology simulation when trying to fit the CO_2 observations (Table 5 and 4). This is also supported by the fact that value of the cost function of the JOINT assimilation roughly equals the sum of the single data-stream experiments, indicating consistency of the model with both data streams.

Hence, although the JSBACH phenology is only weakly influenced by the carbon cycle component of JSBACH and

mainly controlled by other drives (e.g.: soil moisture, temperature), there are strong interactions among carbon and water cycle parameters and simulated FAPAR, a finding supported by Forkel et al. (2014). Thus the combination of different data streams in the JOINT experiment helped estimating parameters of different processes to remain within acceptable bounds. The capability of assimilating multiple data streams simultaneously is a distinct advantage of the MPI-CCDAS over alternative strategies that assimilate multiple data streams by following a sequential design of assimilating FAPAR prior to carbon cycle information. An implementation of such a sequential assimilation likely reduces the number of parameters to be optimized in each step, and therefore allows a quicker solution of the optimisation problem. However, this advantage comes with the cost of breaking the linkage between parameters. ~~This disconnect between the different data streams and their effect on the respective parameter sets~~ can lead to situations, where the posteriori results of a sequential assimilation experiment will not match the observations equally well as with a simultaneous assimilation. Since our results have demonstrated that a joint assimilation is feasible without impairing the fit to the individual data sources, a joint assimilation approach appears therefore recommendable.

The assimilation procedure achieved a strong reduction of the cost function and the norm of the gradient (see Table 3). Although the relative reduction in the norm of the gradient was larger in the CO_2-cases than in the FAPARalone case, the norm did not not approach zero - contrary to the FAPARalone case. Such a non-zero gradient was also noted by Rayner et al. (2005) in their CO_2 assimilation with the BETHY-CCDAS. The fact that the MPI-CCDAS successfully reduces the norm of the gradient for FAPAR suggests that this is not a general failure of the MPI-CCDAS, but specific to the particularities of the CO_2 set-up. It is presently unclear, what is causing the assimilation to fail to reach the minimum of the cost function. ~~, and further tests with alternative station network settings, parameter priors or time-periods are needed to evaluate the cause.~~ Investigation of the non-linear nature and potential numerical issues regarding the computation of the gradient $\frac{\partial J}{\partial p}$ (Eq. 1) might be needed. Further tests with alternative station network settings, parameter priors or time-periods will provide more insight into approaches to tackle this issue. Nevertheless, we believe that our results can still be meaningfully interpreted and used to evaluate the general capacity of the MPI-CCDAS as a comprehensive data assimilation tool.

5.5 Comments on the parameter set-up

The results presented in 4.2 show, that there is a certain degree of equifinality in the parameter values obtained from the assimilation of TIP-FAPAR, as the combination of different parameter values can lead to fairly similar results. This can happen when (i) certain parameters enter an insensitive regime where parameter differences do hardly propagate to differences in the modelled foliar area, (ii) pixels are a composite of different plant functional types that can show compensating effects, and (iii) the CO_2 constraint may still impose an additional weight on changing FAPAR because of the feedbacks on photosynthesis.

Another cautionary note about the posterior parameter values is warranted: Some of the parameters of the JOINT and CO2alone experiment were altered strongly compared to the assumed prior uncertainty. This is possible within the MPI-CCDAS, because the prior contribution to the cost-function is weak due to the small number of parameters compared to the number of observations. One example is the f_{slow} parameter, which controls the initial soil Carbon pool size and thus the disequilibrium between GPP and respiration (Table 2). Another example is the photosynthesis parameter f_{photos} for the tropical evergreen PFT in the JOINT experiment, which was reduced by more than 2.5 times the prior uncertainty and to roughly 75% of its prior value. As a consequence, the assimilation procedure can result in parameter values with small prior probabilities. This either points toward too tight prior uncertainties or to model structural problems.

One such structural problem may be that the current MPI-CCDAS excludes the model spin-up from the assimilation procedure for reasons of computational efficiency: the solution applied was to allow the MPI-CCDAS to manipulate the initial soil carbon pool by one globally valid modifier. This choice was made because allowing to control the spatial structure of the carbon pools would require several more parameters to be optimized, which would very likely suffer from a strong equifinality problem, and which would considerably extend the already lengthy run-time of the MPI-CCDAS. Our results demonstrate that this spin-up approach allows to adequately reproduce the space-time structure of the atmospheric CO_2 budget at the time scale of several years (Fig. 4 and Table 5). However, this approach likely introduces an imprint of the spatial distribution of the prior productivity on the final model outcome, which may cause imperfections in the ability of the MPI-CCDAS to accurately capture the spatial distribution of the net land carbon uptake, and in turn also affect the posteriori parameter vector. Allowing for more spatially explicit modifiers for the initial carbon pools (as is done in the BETHY-CCDAS) by e.g. linking the initial soil disequilibrium to a particular PFT, would be a first step forward.

The stiffness of the MPI-CCDAS respiration parametrisation (with only a few adjustable parameters) likely also caused the reduction of temperate GPP to propagate into the tropical zone, leading to the strong change of f_{photos} for the tropical evergreen PFT in the JOINT experiment. Because the overall net CO_2 flux is constrained by the atmospheric observations, reduction in temperate GPP requires a corresponding adjustment of the ecosystem respiration to balance the budget. While lowering GPP also reduces autotrophic respiration (Eq. A17), any further reduction in respiration

in the temperate zone by adjusting autotrophic (f_{aut_leaf}) or heterotrophic respiration parameters (Q_{10}, f_{slow}) would also affect tropical respiration, because in the current version of the MPI-CCDAS these parameters are assumed to be valid globally. To balance the budget, a reduction in tropical GPP might have been required. Because of enough water availability in the tropics a phase-shift in the dry-wet cycle in the Amazonian rain forest may play a minor role in the down-regulation of GPP during the assimilation. At least no phase mismatch in atmospheric CO_2 is observed at Mauna Loa (Fig. 4) that would suggest such a problem.

~~We also found that extreme parameter changes in vegetation production to better match the observational constraints would impede finding an optimum solution with realistic parameter values. A first series of experiments with the standard maximum foliar area for the coniferous evergreen PFT (not reported here) revealed a bias of 0.4 in FAPAR in the boreal zone. While, in these experiments, the FAPARalone assimilation successfully removed this bias, the lack of a recalculated initial carbon pool meant that the spatial patterns of the initial carbon pools belonging to the high-biased FAPAR values caused compensating effects in the carbon fluxes of other PFTs in the JOINT assimilation run. To avoid this significant bias from affecting our results, the MPI-CCDAS experiments reported here are therefore based on a reduced prior estimate for the coniferous evergreen PFT to account for the sparseness of boreal forests. Strictly speaking this is a violation of the Bayesian theory and a double counting of the information contained in the FAPAR observations. We nevertheless think that this violation is appropriate, as it corrects for a known model shortcoming and since we do not change the prior uncertainties and do not evaluate the posterior probabilities of the parameters.~~

5.6 Further development of the MPI-CCDAS ~~Outlook~~

The application of the MPI-CCDAS allows to detect model structural errors and/or deficits in the set-up, which then can lead to a reformulation of the forward model (see e.g.: Kaminski et al., 2003; Rayner et al., 2005; Williams et al., 2009; Kaminski et al., 2013). The framework described here can be steadily improved through regular improvements of the JSBACH model structure by including missing or correcting false model parametrisations (e.g. Knauer et al., 2015). The system is also versatile enough to add more constraints from relevant and complementary, multiple data sources (Luo et al., 2012) to come up with more robust regional estimates than the current atmospheric inversion allow. Beside the previously discussed limitation related to the spin-up and the representation of initial carbon pools, we can suggest also other analysis and system developments to further improve the MPI-CCDAS.

The discrepancies between FAPARalone and JOINT in the foliar area estimates for crop-dominated regions, even though large in extent, originates from the exclusion of TIP-FAPAR as constraint for these regions. This likewise affected the extra-tropical deciduous PFT, that co-occurred dominantly in the same pixels. Increasing the constraining power of TIP-FAPAR by either adding more pixels as constraints or by increasing the resolution to finer grids might further improve the phenology. ~~We also did not analyse the phenological model behaviour in full detail, because the focus of this work lied on analysing the benefit of the joint assimilation. More focusing on only the FAPAR assimilation also in a spatially more explicit manner could further evaluate the phenology scheme and improve the modelled foliar area.~~ In this context we note that the per-pixel uncertainty ranges in the TIP-FAPAR product also reflect limitations of the information content that can be derived from sunlight reflected to space in the optical domain (i.e. the input to TIP) in particular over dense canopies. Formal uncertainty propagation can quantify the information content in the FAPAR product on gross-fluxes or, conversely, derive accuracy requirments for optical products (Kaminski et al., 2012)

~~We have demonstrated that the JSBACH model is capable of reproducing the seasonal cycle and 5 year trend of the observed atmospheric CO_2 (Fig.s 4 and 5 and Table 5). We have applied a careful selection of stations to avoid the impact of local sources on modelled atmospheric CO_2 mole fractions, which cannot be simulated with the current coarse resolution of the MPI-CCDAS. Nevertheless, the evaluation with the cross-validation sites demonstrates a good skill of the posterior model also for these sites, suggesting that the observed CO_2 dynamics at monthly to yearly time scales are reasonably well captured. Our study supports earlier findings that despite some constraint on Northern extra-tropic production, the constraint of observed atmospheric CO_2 on global production is small (Koffi et al., 2012). It further also supports the studies of Rayner et al. (1999), Kaminski et al. (1999) and Peylin et al. (2013) that the observational network of atmospheric CO_2 only constrains the net carbon fluxes of larger regions.~~

We demonstrated the value of using a CCDAS instead of a pure atmospheric inversion to estimate the land net carbon flux, because the CCDAS can ingest complementary data streams, which may help to further constrain the regional estimates of the net land carbon flux. In this first version of the MPI-CCDAS, we have assumed the net fluxes other than those simulated with JSBACH (i.e. fossil fuel emissions and ocean exchange), as well as the atmospheric drivers to JSBACH to be perfectly known, and thus impute all the model-data mismatch on shortcomings of the land-surface model. It would be desirable to also account for the uncertainties in these components of the modelling system to more robustly identify potential model shortcomings. Further assessing the relative importance of different error sources (e.g. in the land cover type parameterization, model biases or observational errors) with a system such as the MPI-CCDAS would allow to highlight priority areas to reduce their uncertainties and

further constrain the global carbon cycle numbers as given in table 6

Our results show that applying FAPAR and atmospheric CO_2 as a constraint for the JSBACH model leads to an improved simulation of phenology and ~~N~~northern extra-tropical GPP. As a consequence of the assimilation procedure, the model also captures the magnitude of the global and hemispheric net biome exchange. This is a major step forward to including better constrained terrestrial models for the estimation of the global carbon budget (Le Quéré et al., 2015). However, we have set up the model such that it attributes the difference between prior and posterior sink (i.e. 2.2 $PgCyr^{-1}$) to the soil carbon storage. It has been long known that the terrestrial net carbon uptake, and thus the CO_2 signal seen by the atmospheric observations, is strongly affected by natural (such as fire) and anthropogenic disturbances (such as land-use change; Houghton et al. 2012). These processes contribute to the disequilibrium of vegetation and soil carbon pools with vegetation production, and thus affect the spatial pattern of terrestrial carbon release and uptake. Without consideration of these processes, one should be careful in analysing the MPI-CCDAS projected carbon cycle trends and attribution of drivers of the trends. The tangent-linear version of the JSBACH model contained in the MPI-CCDAS already has the appropriate modules to simulate disturbance by fire (Lasslop et al., 2014) and land-use (Reick et al., 2013). A further development of the MPI-CCDAS could be to activate these processes. In order to improve on the current situation it might also be desirable to constrain the post-disturbance dynamics of the carbon pools or at least to analyse how well these are constrained. This would also allow to add more data streams to potentially disentangle the tight parameter linkages in the model.

6 Conclusions

The assimilation of five years of remotely sensed FAPAR and atmospheric CO_2 observations with the MPI-CCDAS was generally successful in that the fairly substantial model-data mismatch of the prior model was largely reduced. The assimilation procedure strongly reduced the too large prior-estimate of GPP, and generally led to an improvement of the simulated carbon cycle and its seasonality. The resultant carbon cycle estimates compared favourably to independent data-driven estimates, although tropical productivity was lower than these estimates. The posterior global net land-atmosphere flux was well constrained and commensurate with independent estimates of the global carbon budget. Our analysis of the prognostic fluxes for a consecutive 2-year period as well as at stations withheld from the assimilation procedure demonstrates that our results are robust.

The factorial inclusion of FAPAR and atmospheric CO_2 as a constraint clearly demonstrated that the two data streams can be simultaneously integrated with the MPI-CCDAS. We have shown the potential of multiple-data-stream assimilation by adding TIP-FAPAR as a constraint and have shown how this data stream helps constraining the foliar area without degrading the ability of the model to capture seasonal and yearly dynamics of the atmospheric CO_2 mole fractions. However, the multi-data assimilation also pointed to model structural problems in the initialisation, which need to be addressed. Nevertheless, our study highlights the potential of adding new data streams to constrain different processes in a global ecosystem model.

This study thus provides an important step forward in the development of global atmospheric inversion schemes~~,~~. ~~by a~~Adding a process-based component, belonging to a coupled carbon-cycle climate model, allows to disentangle the drivers of the terrestrial carbon balance. ~~and~~It also gives the opportunity to apply multiple data streams to constrain ~~them~~ these drivers. ~~in the framework of a land surface model belonging to a coupled carbon-cycle climate model.~~ On the one hand improving the assimilation system and on the other hand adding more data streams can ultimately lead to regionally constrained estimates of the terrestrial carbon balance for the assessment of current and future trends.

Code availability

The JSBACH model code is available upon request to S. Zaehle (soenke.zaehle@bgc-jena.mpg.de)

The TM3 model code is available upon request to to C. Rödenbeck (christian.roedenbeck@bgc-jena.mpg.de)

The TAF generated derivative code is subject to license restrictions and not available.

Appendix A: Model description of JSBACH

A1 The phenology module

A2 ~~Phenology-module~~

In the revised MPI-CCDAS phenology scheme (Knorr et al., 2010), each plant functional type is assigned to a specific phenotype, implying limitations on phenology by water (tropical and raingreen PFTs), water and temperature (herbaceous PFTs) and temperature and daylight (extra-tropical tree PFTs; see Table 1). The evolution of the leaf area index Λ (LAI) on a daily time-step Δt is described as

$$\Lambda(t+\Delta t) = \Lambda_{lim} - [\Lambda_{lim} - \Lambda(t)]e^{-r\Delta t} \quad \text{(A1)}$$

with the inverse time scale r, which is defined as:

$$r = \xi f + (1-f)/\tau_l \quad \text{(A2)}$$

The parameter ξ describes the rate of initial leaf growth, and the parameter τ_l describes how quickly leafs are shed. f spec-

ifies the stage of the vegetation being fully active at $f = 1$ or fully dormant at $f = 0$ (see Eq. A4). Λ_{lim} is defined as:

$$\Lambda_{lim} = \xi \Lambda_{max} f/r \tag{A3}$$

where the parameter Λ_{max} is the maximum allowed LAI.

The scheme accounts for ~~grid-cell~~ naturally occuring heterogeneity within the area of a model grid-cell by smoothly varying the vegetation's state f between the two extremes. The transition is controlled either by the length of the day t_d or a ~~smoothly~~ temporally averaged temperature T_m with exponentially decaying weights for older periods with a ~~a "memory"~~ time scale of 30 days (for details see Knorr et al. (2010)).

$$f = \Phi\left(\frac{T_m - T_\phi}{T_r}\right)\Phi\left(\frac{t_d - t_c}{t_r}\right) \tag{A4}$$

with the temperature control parameters T_ϕ, T_r and day-length control parameters t_c and t_r and the cumulative normal distribution Φ (with mean T_m resp. t_d and standard deviation T_r resp. t_r) .

Water limitation is incorporated by calculating a water-limited maximum leaf area index Λ_W that cannot be exceeded by the actual LAI:

$$\Lambda_W = \frac{W\Lambda^{last}}{E_{pot}\tau_W} \tag{A5}$$

with a water limitation time scale τ_W. The potential evaporation E_{pot}, the relative root-zone moisture W and the LAI Λ^{last} are taken from the previous day averages. Λ_W ~~is also applied with a memory time-scale of 30 days,~~ itself is a temporally averaged LAI with exponentially decaying weigths of 30 day time-scale, similar to temperature and day length above.

A3 Photosynthesis

Photosynthesis in JSBACH follows Farquhar et al. (1980) for C3-plants and Collatz et al. (1992) for C4- plants, with details as described in Knorr and Heimann (2001) and Knorr (1997). Net leaf CO_2 uptake is the minimum of a carboxylation limited photosynthesis rate J_C and of electron transport limited rate J_E minus dark respiration R_d:

$$A = \min(J_C, J_E) - R_d \tag{A6}$$

The carboxylation limited rate is calculated as:

$$J_C = V_m \frac{C_i - \Gamma_\star}{C_i + K_C(1 + O_x/K_O)} \tag{A7}$$

with the leaf internal CO_2-Concentration C_i, the oxygen concentration O_x (0.21 mol/mol) and the CO_2 compensation point (without dark respiration) $\Gamma_\star = 1.7\mu\text{mol/mol}°\text{C} \cdot T$ which depends on temperature T (in °C). K_C and K_O are the Michealis-Menten constants for CO_2 and O_2 and V_m is the maximum carboxylation rate. The latter three all depend on the canopy temperature T_c (in K) in the form (exemplified ~~for~~ by V_m):

$$V_m = Vc_{max} \cdot \exp\left(\frac{E_V T_0}{T_1 R_g T_c}\right) \tag{A8}$$

with activation energy $E_V = 58520$ Jmol^{-1} ~~,~~and gas constant $R_g = 8.314$ JK^{-1}mol^{-1}. $T_1 = 298.16$ °C is a reference temperature and $T_0 = T_c - T_1$ the difference to this reference. Vc_{max} is the maximal carboxylation rate at 25 °C and is given in Table D1. Temperature dependence of K_C and K_O are calculated with a similar approach with reference values at 25 °C for $K_{C0} = 460 \cdot 10^{-6}$ mol/mol and $K_{O0} = 330 \cdot 10^{-3}$ mol/mol and activation energies of $E_C = 59356$ Jmol^{-1} and $E_O = 35948$ Jmol^{-1}, respectively.

The electron transport limited rate, J_E, is calculated as

$$J_E = J\frac{C_i - \Gamma_\star}{4\,(C_i - 2\Gamma_\star)} \tag{A9}$$

with the photon capture efficiency $\alpha = 0.28$ mol(electrons)/mol(photons), the absorption rate of photosynthetically active radiation I, and with

$$J = \frac{\alpha I J_m}{\sqrt{J_m^2 + \alpha^2 I^2}}. \tag{A10}$$

~~and the photon capture efficiency $\alpha = 0.28$ mol(electrons)/mol(photons), the absorption rate of photosynthetically active radiation I, and the limiting rate constant J_m with a temperature dependence:~~ The limiting rate constant J_m depends on the temperature with a maximum rate of electron transport J_{max} at 25 °C (Table D1):

$$J_m = J_{max} \cdot T/25°C \tag{A11}$$

~~J_{max} is the maximum rate of electron transport at 25 °C (Table D1)~~.

Photosynthesis for C4-plants follows Collatz et al. (1992) and is the minimum among the three limiting rates $J_e = V_m$, $J_c = kC_i$ and $J_i = \alpha_i I$ with the quantum efficiency $\alpha_i = 0.04$ and k:

$$k = J_{max} \cdot 10^3 \exp\left(\frac{E_K T_0}{T_1 R_g T_c}\right) \tag{A12}$$

with $E_K = 50967$ Jmol^{-1}.

Dark respiration is modelled depending on Vc_{max} according to

$$R_d = fr_{C3|C4} Vc_{max} \cdot \exp\left(\frac{E_R T_0}{T_1 R_g T_c}\right) \tag{A13}$$

with activation energy $E_R = 45000$ Jmol^{-1}, and $fr_{C3|C4} = 0.011|0.031$ for C3 and C4 plants, respectively. Dark respiration is reduced to 50% of its value during light conditions (Brooks and Farquhar, 1985).

Photosynthesis and dark respiration are inhibited above 55°C. Calculations are performed per PFT and three distinct canopy layers, which vary in depth according to the current leaf area index, assuming that within the canopy nitrogen, and thus Vc_{max}, J_{max}, and R_d decline proportionally with light levels in the canopy. GPP - values per PFT ~~values~~ are integrated to grid-cell averages according to the cover fractions of each PFT within each grid-cell.

A4 Carbon-water coupling

JSBACH employs a two-step approach to couple the plant carbon and water fluxes (Knauer et al., 2015). Given a photosynthetic-pathway dependent specific maximal internal leaf CO_2 concentration (C_i), a maximal estimate of stomatal conductance (gs_{pot}) is derived for each canopy layer, which is then reduced by a water-stress factor (w_s) to arrive at the actual stomatal conductance (gs_{act}) (see Knorr, 1997, 2000, and references therein).

$$gs_{act} = w_s \cdot gs_{pot} = w_s \cdot 1.6 \cdot \frac{A}{C_a - C_i} \tag{A14}$$

where C_a and C_i are the external and internal leaf CO_2 concentrations. The water-stress factor w_s is defined as

$$w_s = \min\left(\frac{W_{root} - W_{wilt}}{W_{crit} - W_{wilt}}, 1\right) \tag{A15}$$

where W_{root} is the actual soil-moisture in the root zone, and $W_{crit|wilt}$ define the soil moisture levels at which stomata begin to close, or reach full closure, respectively. Soil moisture and bare soil evaporation are calculated according to the multi-layer soil water scheme of Hagemann and Stacke (2014).

Given the water-stressed stomatal conductance, leaf internal CO_2 concentration and carbon assimilation are then recalculated for each canopy layer by solving simultaneously the diffusion equation (Eq. A14) and the photosynthesis equations as outlined above (Sec. A3)

A5 Land carbon pools, respiration and turnover

The vegetation's net primary production (NPP) is related to the net assimilation (A) as

$$NPP = A - R_m - R_g \tag{A16}$$

where R_g is the growth respiration, which is assumed to be a fixed fraction (20%) of $A - R_m$. R_m is the maintenance respiration, which is assumed to be coordinated with foliar photosynthetic activity, and thus scaled to leaf dark respiration via f_{aut_leaf} (Knorr, 2000)

$$R_m = \frac{R_d}{f_{aut\_leaf}} \tag{A17}$$

with the dark respiration R_d as given in Eq. A13. As a consequence, an increase in f_aut_leaf leads to an increase in NPP.

NPP is allocated to either a green or woody pool given fixed, PFT-specific allocation constants. The green pool turns ~~over~~ to litter according to the leaf phenology, whereas the woody turnover rate is prescribed as a fixed constant.

JSBACH considers three litter pools (above ground green, below ground green and woody) with distinct, PFT-specific turnover times, as well as a soil organic matter pool with a longer turnover time. Heterotrophic respiration for each of these pools responds to temperature according to a Q_{10} formulation:

$$R_{pool} = \alpha_{resp} Q_{10}^{(T - T_{ref})/10} / \tau_{pool} \cdot C_{pool} \tag{A18}$$

with a soil-moisture dependent factor $0 <= \alpha_{resp} <= 1$. C_{pool} is either the slow soil carbon pool, above or below ground green litter or wood litter pool and T is temperature and $T_{ref} = 0°C$ the reference temperature and a pool depended turnover rate τ_{pool} (more details on the carbon balance sub-module can be found in Goll et al., 2012).

Appendix B: CO_2 station list

The stations of atmospheric CO_2-observations used for assimilation and evaluation are given in Table B1 resp. Table B2.

Appendix C: Mapping variants

For performance reasons, the assimilation is not performed in the physical parameter space but parameters p are transformed to x expressed in multiples of the prior uncertainty, the intrinsic units of the problem (Kaminski et al., 1999). The most basic mapping is:

$$x = \frac{p - p_0}{\sigma_{prior}} \qquad \Leftrightarrow \qquad p = p_0 + x\sigma_{prior} \tag{C1}$$

An extension of this is to apply lower bounds in the mapping back to physical space with

$$\begin{aligned} p &= p_{min} + x_{low}/x\sigma_{prior} \\ &\text{only if} \\ x &< x_{low} = \frac{p_{min} + \sigma_{prior} - p_0}{\sigma_{prior}} \end{aligned} \tag{C2}$$

with p_{min} the minimum allowed parameter value.

Appendix D: Parameter values

Some parameters were modified with a factor within the MPI-CCDAS, because model structure did not allow to di-

Table B1. CO_2 stations used in the assimilation together with their median uncertainty.

ID	Longitude	Latitude	Median Uncertainty
MNM	153.97	24.30	1.4
SBL	-60.02	43.93	5.9
ALT	-62.52	82.45	1.8
ASC	-14.42	-7.92	1.1
AZR	-27.19	38.76	1.9
BHD	174.90	-41.40	1.0
CHR	-157.17	1.70	1.0
CRZ	51.85	-46.45	1.0
EIC	-109.45	-27.15	1.1
ESP	-126.83	49.56	2.9
GMI	144.78	13.43	1.2
HBA	-26.65	-75.58	1.0
ICE	-20.21	63.30	1.9
KER	-177.15	-29.03	1.0
KUM	-154.82	19.52	1.6
MHD	-9.90	53.33	2.4
MID	-177.37	28.22	1.7
MQA	158.97	-54.48	1.0
RPB	-59.43	13.17	1.1
SEY	55.17	-4.67	1.0
SHM	174.10	52.72	2.1
SIS	-1.23	60.23	3.1
STM	2.00	66.00	3.2
TDF	-68.48	-54.87	1.0
ZEP	11.88	78.90	2.3
MLO	-155.58	19.53	1.1
SMO	-170.57	-14.25	1.0
SPO	-24.80	-89.98	1.0

rectly change these values and thus such an approach was required. The parameter values are listed in Table D1.

Appendix E: PFT-distribution

The vegetation distribution of the PFT's as prescribed in the MPI-CCDAS is given in Fig. E1.

Table B2. CO_2 stations used for evaluation that have not been used as constraints for the assimilation.

ID	Longitude	Latitude
PAL	24.12	67.97
PRS	7.70	45.93
RYO	141.83	39.03
YON	123.02	24.47
CBA	-162.72	55.20
CFA	147.06	-19.28
CGO	144.70	-40.68
COI	145.50	43.15
CYA	110.52	-66.28
HAT	123.80	24.05
IZO	-16.48	28.30
KEY	-80.20	25.67
LEF	-90.27	45.93
LJO	-117.25	32.87
LMP	12.61	35.51
MAA	62.87	-67.62
NWR	-105.60	40.05
PSA	-64.00	-64.92
SUM	-38.47	72.57
TAP	126.13	36.73
UTA	-113.72	39.90
UUM	111.10	44.45
WIS	34.88	31.13
WLG	100.91	36.28
BRW	-156.60	71.32
SYO	39.58	-69.00
CMN	10.70	44.18
SCH	7.92	47.92

Table D1. Values of those parameters that have been changed with a multiplicative factor during the assimilation.

PFT	TrBE	TrBD	ETD	CE	CD	RS	TeH	TeCr	TrH	TrCr
Prior Λ_{max} [m^2/m^2]	7.0	7.0	5.0	1.7	5.0	2.0	3.0	4.0	3.0	4.0
Joint Λ_{max} [m^2/m^2]	6.9	4.1	4.9	1.7	3.2	2.7	1.9	2.5	1.6	2.1
Prior Vc_{max} [µmol/m^2s]	39.0	31.0	66.0	62.5	39.1	61.7	78.2	100.7	8.0	39.0
Joint Vc_{max} [µmol/m^2s]	29.2	33.3	65.1	59.2	40.6	62.1	75.4	67.9	8.3	34.1
Prior J_{max} [µmol/m^2s]	74.1	58.9	125.4	118.8	74.3	117.2	148.6	191.3	140.0	700.0
Joint J_{max} [µmol/m^2s]	55.5	63.3	123.7	112.5	77.2	117.9	143.2	129.0	145.0	611.2

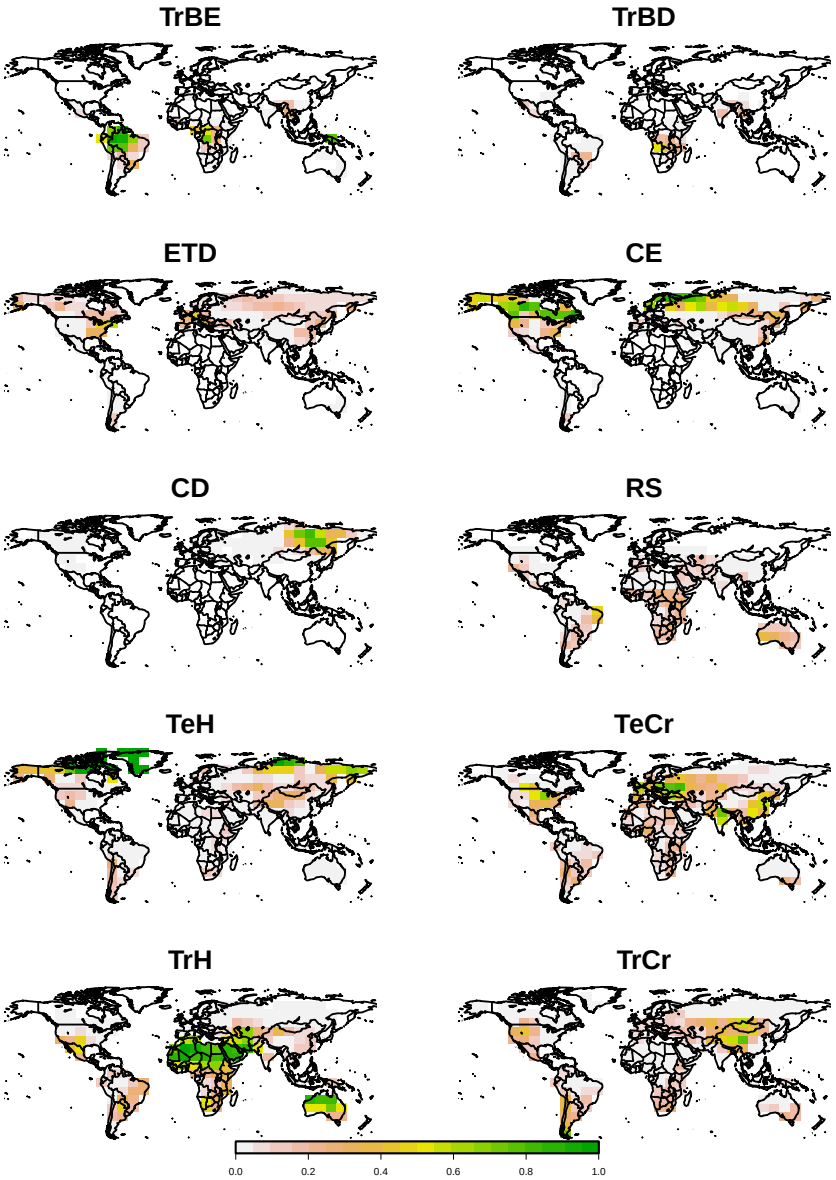

Figure E1. Fractional vegetation coverage of the PFT's as prescribed in the MPI-CCDAS. See Table 1 for abbreviations.

Acknowledgements. The research leading to this publication was supported by the European Space Agency through the STSE Carbonflux (contract no. 4000107086/12/NL/Fv0), the European Community within its 7th framework programme under contract number (GEOCARBON; FP7-283080), as well as the Max Planck Society for the Advancement of Science, e.V. through the ENIGMA project. The authors thank P. Peylin for providing the fossil fuel emission data, M. Scholze, W. Knorr and K. Scipal for fruitful discussions and C. Reick, R. Schnur and V. Gayler for assistance with the JSBACH model.

References

Anav, A., Friedlingstein, P., Kidston, M., Bopp, L., Ciais, P., Cox, P., Jones, C., Jung, M., Myneni, R., and Zhu, Z.: Evaluating the Land and Ocean Components of the Global Carbon Cycle in the CMIP5 Earth System Models, J. Climate, 26, 6801–6843, 2013.

Bacour, C., Peylin, P., MacBean, N., Rayner, P. J., Delage, F., Chevallier, F., Weiss, M., Demarty, J., Santaren, D., Baret, F., Berveiller, D., Dufrêne, E., and Prunet, P.: Joint assimilation of eddy covariance flux measurements and FAPAR products over temperate forests within a process-oriented biosphere model, Journal of Geophysical Research: Biogeosciences, 120, 1839–1857, doi:10.1002/2015JG002966, http://dx.doi.org/10.1002/2015JG002966, 2015JG002966, 2015.

Beer, C., Reichstein, M., Tomelleri, E., Ciais, P., Jung, M., Carvalhais, N., Rödenbeck, C., Arain, M. A., Baldocchi, D., Bonan, G. B., Bondeau, A., Cescatti, A., Lasslop, G., Lindroth, A., Lomas, M., Luyssaert, S., Margolis, H., Oleson, K. W., Roupsard, O., Veenendaal, E., Viovy, N., Williams, C., Woodward, F. I., and Papale, D.: Terrestrial Gross Carbon Dioxide Uptake: Global Distribution and Covariation with Climate, Science, 329, 834–838, doi:10.1126/science.1184984, 2010.

Booth, B. B. B., Jones, C. D., Collins, M., Totterdell, I. J., Cox, P. M., Sitch, S., Huntingford, C., Betts, R. A., Harris, G. R., and Lloyd, J.: High sensitivity of future global warming to land carbon cycle processes, Environmental Research Letters, 7, 024 002, 2012.

Brooks, A. and Farquhar, G.: Effect of temperature on the CO2/O2 specificity of ribulose-1,5-bisphosphate carboxylase/oxygenase and the rate of respiration in the light, Planta, 165, 397–406, doi:10.1007/BF00392238, 1985.

Brovkin, V., Raddatz, T., Reick, C. H., Claussen, M., and Gayler, V.: Global biogeophysical interactions between forest and climate, Geophysical Research Letters, 36, doi:10.1029/2009GL037543, 2009.

Carvalhais, N., Reichstein, M., Seixas, J., Collatz, G. J., Pereira, J. S., Berbigier, P., Carrara, A., Granier, A., Montagnani, L., Papale, D., Rambal, S., Sanz, M. J., and Valentini, R.: Implications of the carbon cycle steady state assumption for biogeochemical modeling performance and inverse parameter retrieval, Global Biogeochemical Cycles, 22, n/a–n/a, doi:10.1029/2007GB003033, http://dx.doi.org/10.1029/2007GB003033, gB2007, 2008.

Carvalhais, N., Forkel, M., Khomik, M., Bellarby, J., Jung, M., Migliavacca, M., Mu, M., Saatchi, S., Santoro, M., Thurner, M., Weber, U., Ahrens, B., Beer, C., Cescatti, A., Randerson, J. T., and Reichstein, M.: Global covariation of carbon turnover times with climate in terrestrial ecosystems, Nature, 514, 213–217, 2014.

Clerici, M., Vossbeck, M., Pinty, B., Kaminski, T., Taberner, M., Lavergne, T., and Andredakis, I.: Consolidating the Two-Stream Inversion Package (JRC-TIP) to Retrieve Land Surface Parameters From Albedo Products, Selected Topics in Applied Earth Observations and Remote Sensing, IEEE Journal of, 3, 286–295, doi:10.1109/JSTARS.2010.2046626, 2010.

Collatz, G., Ribas-Carbo, M., and Berry, J.: Coupled Photosynthesis-Stomatal Conductance Model for Leaves of C_4 Plants, Functional Plant Biol., 19, 519–538, 1992.

Conway, T. J., Tans, P. P., Waterman, L. S., Thoning, K. W., Kitzis, D. R., Masarie, K. A., and Zhang, N.: Evidence for interannual variability of the carbon cycle from the National Oceanic and Atmospheric Administration/Climate Monitoring and Diagnostics Laboratory Global Air Sampling Network, Journal of Geophysical Research: Atmospheres, 99, 22 831–22 855, doi:10.1029/94JD01951, 1994.

Cramer, W., Kicklighter, D. W., Bondeau, A., Iii, B. M., Churkina, G., Nemry, B., Ruimy, A., Schloss, A. L., and Intercomparison, T. P. O. T. P. N. M.: Comparing global models of terrestrial net primary productivity (NPP): overview and key results, Global Change Biology, 5, 1–15, doi:10.1046/j.1365-2486.1999.00009.x, 1999.

Dalmonech, D. and Zaehle, S.: Towards a more objective evaluation of modelled land-carbon trends using atmospheric CO_2 and satellite-based vegetation activity observations, Biogeosciences, 10, 4189–4210, doi:10.5194/bg-10-4189-2013, 2013.

Dalmonech, D., Zaehle, S., Schürmann, G. J., Brovkin, V., Reick, C., and Schnur, R.: Separation of the Effects of Land and Climate Model Errors on Simulated Contemporary Land Carbon Cycle Trends in the MPI Earth System Model version 1, J. Climate, 28, 272–291, 2015.

Disney, M., Muller, J.-P., Kharbouche, S., **Kaminski**, **Thomas**., **Voßbeck**, **Michael**., Lewis, P., and Pinty, B.: A New Global fAPAR and LAI Dataset Derived from Optimal Albedo Estimates: Comparison with MODIS Products, Remote Sensing, 8, 275, doi:10.3390/rs8040275, http://www.mdpi.com/2072-4292/8/4/275, 2016.

European Commission, Joint Research Centre (JRC)/Netherlands Environmental Assessment Agency (PBL): Emission Database for Global Atmospheric Research (EDGAR), release version 4.0, http://edgar.jrc.ec.europa.eu,2009, 2009.

Farquhar, G., von Caemmerer, S., and Berry, J.: A biochemical model of photosynthetic CO2 assimilation in leaves of C3 species, Planta, 149, 78–90, doi:10.1007/BF00386231, 1980.

Forkel, M., Carvalhais, N., Schaphoff, S., v. Bloh, W., Migliavacca, M., Thurner, M., and Thonicke, K.: Identifying environmental controls on vegetation greenness phenology through model–data integration, Biogeosciences, 11, 7025–7050, doi:10.5194/bg-11-7025-2014, 2014.

Friedlingstein, P., Meinshausen, M., Arora, V. K., Jones, C. D., Anav, A., Liddicoat, S. K., and Knutti, R.: Uncertainties in CMIP5 Climate Projections due to Carbon Cycle Feedbacks, J. Climate, 27, 511–526, 2014.

Giering, R. and Kaminski, T.: Recipes for Adjoint Code Construction, ACM Trans. Math. Softw., 24, 437–474, doi:10.1145/293686.293695, 1998.

Giorgetta, M. A., Jungclaus, J., Reick, C. H., Legutke, S., Bader, J., Böttinger, M., Brovkin, V., Crueger, T., Esch, M., Fieg, K., Glushak, K., Gayler, V., Haak, H., Hollweg, H.-D., Ilyina, T., Kinne, S., Kornblueh, L., Matei, D., Mauritsen, T., Mikolajewicz, U., Mueller, W., Notz, D., Pithan, F., Raddatz, T., Rast, S., Redler, R., Roeckner, E., Schmidt, H., Schnur, R., Segschneider, J., Six, K. D., Stockhause, M., Timmreck, C., Wegner, J., Widmann, H., Wieners, K.-H., Claussen, M., Marotzke, J., and Stevens, B.: Climate and carbon cycle changes from 1850 to 2100 in MPI-ESM simulations for the Coupled Model Intercomparison Project phase 5, Journal of Advances in Modeling Earth Systems, 5, 572–597, doi:10.1002/jame.20038, 2013.

Gobron, N., Pinty, B., Melin, F., Taberner, M., Verstraete, M. M., Robustelli, M., and Widlowski, J.-L.: Evaluation of the MERIS/ENVISAT FAPAR product, Adv. Space Res., 39, 105–115, 2007.

Goll, D. S., Brovkin, V., Parida, B. R., Reick, C. H., Kattge, J., Reich, P. B., van Bodegom, P. M., and Niinemets, U.: Nutrient limitation reduces land carbon uptake in simulations with a model of combined carbon, nitrogen and phosphorus cycling, Biogeosciences, 9, 3547–3569, doi:10.5194/bg-9-3547-2012, 2012.

Griewank, A.: On Automatic Differentiation, in: Mathematical Programming: Recent Developments and Applications, edited by Iri, M. and Tanabe, K., pp. 83–108, Kluwer Academic Publishers, Dordrecht, 1989.

Gurney, K. R., Law, R. M., Denning, A. S., Rayner, P. J., Baker, D., Bousquet, P., Bruhwiler, L., Chen, Y.-H., Ciais, P., Fan, S., Fung, I. Y., Gloor, M., Heimann, M., Higuchi, K., John, J., Maki, T., Maksyutov, S., Masarie, K., Peylin, P., Prather, M., Pak, B. C., Randerson, J., Sarmiento, J., Taguchi, S., Takahashi, T., and Yuen, C.-W.: Towards robust regional estimates of CO2 sources and sinks using atmospheric transport models, Nature, 415, 626–630, 2002.

Hagemann, S. and Stacke, T.: Impact of the soil hydrology scheme on simulated soil moisture memory, Climate Dynamics, pp. 1–20, doi:10.1007/s00382-014-2221-6, 2014.

Heimann, M. and Körner, S.: The Global Atmospheric Tracer Model TM3, Tech. Rep. 5, Max-Planck-Institute for Biogeochemistry, 2003.

Houghton, R. A., House, J. I., Pongratz, J., van der Werf, G. R., DeFries, R. S., Hansen, M. C., Le Quéré, C., and Ramankutty, N.: Carbon emissions from land use and land-cover change, Biogeosciences, 9, 5125–5142, doi:10.5194/bg-9-5125-2012, 2012.

Jacobson, A. R., Mikaloff Fletcher, S. E., Gruber, N., Sarmiento, J. L., and Gloor, M.: A joint atmosphere-ocean inversion for surface fluxes of carbon dioxide: 1. Methods and global-scale fluxes, Global Biogeochemical Cycles, 21, n/a–n/a, doi:10.1029/2005GB002556, http://dx.doi.org/10.1029/2005GB002556, gB1019, 2007.

Jung, M., Vetter, M., Herold, M., Churkina, G., Reichstein, M., Zaehle, S., Ciais, P., Viovy, N., Bondeau, A., Chen, Y., Trusilova, K., Feser, F., and Heimann, M.: Uncertainties of modeling gross primary productivity over Europe: A systematic study on the effects of using different drivers and terrestrial biosphere models, Global Biogeochemical Cycles, 21, n/a–n/a, doi:10.1029/2006GB002915, gB4021, 2007.

Jung, M., Reichstein, M., Margolis, H. A., Cescatti, A., Richardson, A. D., Arain, M. A., Arneth, A., Bernhofer, C., Bonal, D., Chen, J., Gianelle, D., Gobron, N., Kiely, G., Kutsch, W., Lasslop, G., Law, B. E., Lindroth, A., Merbold, L., Montagnani, L., Moors, E. J., Papale, D., Sottocornola, M., Vaccari, F., and Williams, C.: Global patterns of land-atmosphere fluxes of carbon dioxide, latent heat, and sensible heat derived from eddy covariance, satellite, and meteorological observations, Journal of Geophysical Research: Biogeosciences, 116, n/a–n/a, doi:10.1029/2010JG001566, 2011.

Kalnay, E., Kanamitsu, M., Kistler, R., Collins, W., Deaven, D., Gandin, L., Iredell, M., Saha, S., White, G., Woollen, J., Zhu, Y., Leetmaa, A., Reynolds, R., Chelliah, M., Ebisuzaki, W., Higgins, W., Janowiak, J., Mo, K. C., Ropelewski, C., Wang, J., Jenne, R., and Joseph, D.: The NCEP/NCAR 40-Year Reanalysis Project, Bull. Amer. Meteor. Soc., 77, 437–471, 1996.

Kaminski, T. and Mathieu, P.-P.: Reviews and Syntheses: Flying the Satellite into Your Model, Biogeosciences Discussions, 2016, 1–25, doi:10.5194/bg-2016-237, http://www.biogeosciences-discuss.net/bg-2016-237/, 2016.

Kaminski, T., Heimann, M., and Giering, R.: A coarse grid three dimensional global inverse model of the atmospheric transport, 2, Inversion of the transport of CO_2 in the 1980s, J. Geophys. Res., 104, 18,555–18,581, 1999.

Kaminski, T., Giering, R., Scholze, M., Rayner, P., and Knorr, W.: A prototype of a data assimilation system based on automatic differentiation, Geophysical Research Abstracts, 5, 11 812, http://www.cosis.net/abstracts/EAE03/11812/EAE03-J-11812.pdf, 2003.

Kaminski, T., Knorr, W., Scholze, M., Gobron, N., Pinty, B., Giering, R., and Mathieu, P.-P.: Consistent assimilation of MERIS FAPAR and atmospheric CO_2 into a terrestrial vegetation model and interactive mission benefit analysis, Biogeosciences, 9, 3173–3184, doi:10.5194/bg-9-3173-2012, 2012.

Kaminski, T., Knorr, W., Schürmann, G., Scholze, M., Rayner, P. J., Zaehle, S., Blessing, S., Dorigo, W., Gayler, V., Giering, R., Gobron, N., Grant, J. P., Heimann, M., Hooker-Stroud, A., Houweling, S., Kato, T., Kattge, J., Kelley, D., Kemp, S., Koffi, E. N., Köstler, C., Mathieu, P.-P., Pinty, B., Reick, C. H., Rödenbeck, C., Schnur, R., Scipal, K., Sebald, C., Stacke, T., van Scheltinga, A. T., Vossbeck, M., Widmann, H., and Ziehn, T.: The BETHY/JSBACH Carbon Cycle Data Assimilation System: experiences and challenges, J. Geophys. Res. Biogeosci., 118, 1414–1426, 2013.

Kato, T., Knorr, W., Scholze, M., Veenendaal, E., Kaminski, T., Kattge, J., and Gobron, N.: Simultaneous assimilation of satellite and eddy covariance data for improving terrestrial water and carbon simulations at a semi-arid woodland site in Botswana, Biogeosciences, 10, 789–802, doi:10.5194/bg-10-789-2013, http://www.biogeosciences.net/10/789/2013/, 2013.

Kattge, J. and Knorr, W.: Temperature acclimation in a biochemical model of photosynthesis: a reanalysis of data from 36 species, Plant, Cell & Environment, 30, 1176–1190, doi:10.1111/j.1365-3040.2007.01690.x, 2007.

Kattge, J., Dí az, S., Lavorel, S., Prentice, I. C., Leadley, P., Bönisch, G., Garnier, E., Westoby, M., Reich, P. B., Wright, I. J., Cornelissen, J. H. C., Violle, C., Harrison, S. P., Van Bodegom, P. M., Reichstein, M., Enquist, B. J., Soudzilovskaia, N. A., Ackerly, D. D., Anand, M., Atkin, O., Bahn, M., Baker, T. R., Baldocchi, D., Bekker, R., Blanco, C. C., Blonder, B., Bond, W. J., Bradstock, R., Bunker, D. E., Casanoves, F., Cavender-Bares, J., Chambers, J. Q., Chapin III, F. S., Chave, J., Coomes,

D., Cornwell, W. K., Craine, J. M., Dobrin, B. H., Duarte, L., Durka, W., Elser, J., Esser, G., Estiarte, M., Fagan, W. F., Fang, J., Fernández-Méndez, F., Fidelis, A., Finegan, B., Flores, O., Ford, H., Frank, D., Freschet, G. T., Fyllas, N. M., Gallagher, R. V., Green, W. A., Gutierrez, A. G., Hickler, T., Higgins, S. I., Hodgson, J. G., Jalili, A., Jansen, S., Joly, C. A., Kerkhoff, A. J., Kirkup, D., Kitajima, K., Kleyer, M., Klotz, S., Knops, J. M. H., Kramer, K., Kühn, I., Kurokawa, H., Laughlin, D., Lee, T. D., Leishman, M., Lens, F., Lenz, T., Lewis, S. L., Lloyd, J., Llusià, J., Louault, F., MA, S., Mahecha, M. D., Manning, P., Massad, T., Medlyn, B. E., Messier, J., Moles, A. T., Müller, S. C., Nadrowski, K., Naeem, S., Niinemets, U., Nöllert, S., Nüske, A., Ogaya, R., Oleksyn, J., Onipchenko, V. G., Onoda, Y., Ordoñez, J., Overbeck, G., Ozinga, W. A., Patiño, S., Paula, S., Pausas, J. G., Peñuelas, J., Phillips, O. L., Pillar, V., Poorter, H., Poorter, L., Poschlod, P., Prinzing, A., Proulx, R., Rammig, A., Reinsch, S., Reu, B., Sack, L., Salgado-Negret, B., Sardans, J., Shiodera, S., Shipley, B., Siefert, A., Sosinski, E., Soussana, J.-F., Swaine, E., Swenson, N., Thompson, K., Thornton, P., Waldram, M., Weiher, E., White, M., White, S., Wright, S. J., Yguel, B., Zaehle, S., Zanne, A. E., and Wirth, C.: TRY – a global database of plant traits, Global Change Biology, 17, 2905–2935, doi:10.1111/j.1365-2486.2011.02451.x, http://dx.doi.org/10.1111/j.1365-2486.2011.02451.x, 2011.

Knauer, J., Werner, C., and Zaehle, S.: Evaluating stomatal models and their atmospheric drought response in a land surface scheme: A multi-biome analysis, Journal of Geophysical Research: Biogeosciences, pp. n/a–n/a, doi:10.1002/2015JG003114, 2015JG003114, 2015.

Knorr, W.: Satellite remote sensing and modelling of the global CO2 exchange of land vegetation: a synthesis study, Ph.D. thesis, Faculty of Earth Sciences of the University of Hamburg, 1997.

Knorr, W.: Annual and interannual CO2 exchanges of the terrestrial biosphere: process-based simulations and uncertainties, Global Ecology and Biogeography, 9, 225–252, 2000.

Knorr, W. and Heimann, M.: Uncertainties in global terrestrial biosphere modeling: 1. A comprehensive sensitivity analysis with a new photosynthesis and energy balance scheme, Global Biogeochemical Cycles, 15, 207–225, doi:10.1029/1998GB001059, 2001.

Knorr, W. and Kattge, J.: Inversion of terrestrial ecosystem model parameter values against eddy covariance measurements by Monte Carlo sampling, Global Change Biology, 11, 1333–1351, doi:10.1111/j.1365-2486.2005.00977.x, 2005.

Knorr, W., Kaminski, T., Scholze, M., Gobron, N., Pinty, B., Giering, R., and Mathieu, P.-P.: Carbon cycle data assimilation with a generic phenology model, J. Geophys. Res., 115, G04 017–, doi:10.1029/2009JG001119, 2010.

Knyazikhin, Y., Glassy, J., Privette, J. L., Tian, Y., Lotsch, A., Zhang, Y., Wang, Y., Morisette, J. T., Votava, P., Myneni, R., Nemani, R. R., and Running, S. W.: MODIS Leaf Area Index (LAI) and Fraction of Photosynthetically Active Radiation Absorbed by Vegetation (FPAR) Product (MOD15), Algorithm Theoretical Basis Document (ATBD), https://lpdaac.usgs.gov/products/modis_products_table/mcd15a2andhttp://modis.gsfc.nasa.gov/data/atbd/atbd_mod15.pdf, 1999.

Koffi, E. N., Rayner, P. J., Scholze, M., and Beer, C.: Atmospheric constraints on gross primary productivity and net ecosystem productivity: Results from a carbon-cycle data assimilation system, Global Biogeochemical Cycles, 26, n/a–n/a, doi:10.1029/2010GB003900, gB1024, 2012.

Kuppel, S., Peylin, P., Chevallier, F., Bacour, C., Maignan, F., and Richardson, A. D.: Constraining a global ecosystem model with multi-site eddy-covariance data, Biogeosciences, 9, 3757–3776, doi:10.5194/bg-9-3757-2012, 2012.

Kuppel, S., Chevallier, F., and Peylin, P.: Quantifying the model structural error in carbon cycle data assimilation systems, Geoscientific Model Development, 6, 45–55, doi:10.5194/gmd-6-45-2013, 2013.

Lasslop, G.: Model data fusion for terrestrial biosphere models with carbon and water cycle observations, Tech. Rep. 20, Max-Planck-Institut für Biogeochemie, P.O.Box 100164, 2011.

Lasslop, G., Thonicke, K., and Kloster, S.: SPITFIRE within the MPI Earth system model: Model development and evaluation, Journal of Advances in Modeling Earth Systems, 6, 740–755, doi:10.1002/2013MS000284, 2014.

Le Quéré, C., Moriarty, R., Andrew, R. M., Peters, G. P., Ciais, P., Friedlingstein, P., Jones, S. D., Sitch, S., Tans, P., Arneth, A., Boden, T. A., Bopp, L., Bozec, Y., Canadell, J. G., Chini, L. P., Chevallier, F., Cosca, C. E., Harris, I., Hoppema, M., Houghton, R. A., House, J. I., Jain, A. K., Johannessen, T., Kato, E., Keeling, R. F., Kitidis, V., Klein Goldewijk, K., Koven, C., Landa, C. S., Landschützer, P., Lenton, A., Lima, I. D., Marland, G., Mathis, J. T., Metzl, N., Nojiri, Y., Olsen, A., Ono, T., Peng, S., Peters, W., Pfeil, B., Poulter, B., Raupach, M. R., Regnier, P., Rödenbeck, C., Saito, S., Salisbury, J. E., Schuster, U., Schwinger, J., Séférian, R., Segschneider, J., Steinhoff, T., Stocker, B. D., Sutton, A. J., Takahashi, T., Tilbrook, B., van der Werf, G. R., Viovy, N., Wang, Y.-P., Wanninkhof, R., Wiltshire, A., and Zeng, N.: Global carbon budget 2014, Earth System Science Data, 7, 47–85, doi:10.5194/essd-7-47-2015, 2015.

Loew, A., van Bodegom, P. M., Widlowski, J.-L., Otto, J., Quaife, T., Pinty, B., and Raddatz, T.: Do we (need to) care about canopy radiation schemes in DGVMs? Caveats and potential impacts, Biogeosciences, 11, 1873–1897, doi:10.5194/bg-11-1873-2014, 2014.

Luke, C. M.: Modelling aspects of land-atmosphere interaction: Thermal instability in peatland soils and land parameter estimation through data assimilation, Ph.D. thesis, University of Exeter, U.K., 2011.

Luo, Y. Q., Randerson, J. T., Abramowitz, G., Bacour, C., Blyth, E., Carvalhais, N., Ciais, P., Dalmonech, D., Fisher, J. B., Fisher, R., Friedlingstein, P., Hibbard, K., Hoffman, F., Huntzinger, D., Jones, C. D., Koven, C., Lawrence, D., Li, D. J., Mahecha, M., Niu, S. L., Norby, R., Piao, S. L., Qi, X., Peylin, P., Prentice, I. C., Riley, W., Reichstein, M., Schwalm, C., Wang, Y. P., Xia, J. Y., Zaehle, S., and Zhou, X. H.: A framework for benchmarking land models, Biogeosciences, 9, 3857–3874, doi:10.5194/bg-9-3857-2012, 2012.

Mahecha, M. D., Reichstein, M., Carvalhais, N., Lasslop, G., Lange, H., Seneviratne, S. I., Vargas, R., Ammann, C., Arain, M. A., Cescatti, A., Janssens, I. A., Migliavacca, M., Montagnani, L., and Richardson, A. D.: Global Convergence in the Temperature Sensitivity of Respiration at Ecosystem Level, Science, 329, 838–840, doi:10.1126/science.1189587, http://science.sciencemag.org/content/329/5993/838, 2010.

Peylin, P., Law, R. M., Gurney, K. R., Chevallier, F., Jacobson, A. R., Maki, T., Niwa, Y., Patra, P. K., Peters, W., Rayner,

P. J., Rödenbeck, C., van der Laan-Luijkx, I. T., and Zhang, X.: Global atmospheric carbon budget: results from an ensemble of atmospheric CO_2 inversions, Biogeosciences, 10, 6699–6720, doi:10.5194/bg-10-6699-2013, 2013.

Piao, S., Sitch, S., Ciais, P., Friedlingstein, P., Peylin, P., Wang, X., Ahlström, A., Anav, A., Canadell, J. G., Cong, N., Huntingford, C., Jung, M., Levis, S., Levy, P. E., Li, J., Lin, X., Lomas, M. R., Lu, M., Luo, Y., Ma, Y., Myneni, R. B., Poulter, B., Sun, Z., Wang, T., Viovy, N., Zaehle, S., and Zeng, N.: Evaluation of terrestrial carbon cycle models for their response to climate variability and to CO2 trends, Global Change Biology, 19, 2117–2132, doi:10.1111/gcb.12187, 2013.

Pinty, B., Lavergne, T., Dickinson, R., Widlowski, J., Gobron, N., and Verstraete, M.: Simplifying the interaction of land surfaces with radiation for relating remote sensing products to climate models, J. Geophys. Res, 2006.

Pinty, B., Lavergne, T., Voßbeck, M., Kaminski, T., Aussedat, O., Giering, R., Gobron, N., Taberner, M., Verstraete, M. M., and Widlowski, J.-L.: Retrieving surface parameters for climate models from Moderate Resolution Imaging Spectroradiometer (MODIS)-Multiangle Imaging Spectroradiometer (MISR) albedo products, Journal of Geophysical Research: Atmospheres, 112, n/a–n/a, doi:10.1029/2006JD008105, http://dx.doi.org/10.1029/2006JD008105, d10116, 2007.

Pinty, B., Andredakis, I., Clerici, M., Kaminski, T., Taberner, M., Verstraete, M. M., Gobron, N., Plummer, S., and Widlowski, J.-L.: Exploiting the MODIS albedos with the Two-stream Inversion Package (JRC-TIP): 1. Effective leaf area index, vegetation, and soil properties, Journal of Geophysical Research: Atmospheres, 116, n/a–n/a, doi:10.1029/2010JD015372, 2011a.

Pinty, B., Clerici, M., Andredakis, I., Kaminski, T., Taberner, M., Verstraete, M. M., Gobron, N., Plummer, S., and Widlowski, J.-L.: Exploiting the MODIS albedos with the Two-stream Inversion Package (JRC-TIP): 2. Fractions of transmitted and absorbed fluxes in the vegetation and soil layers, Journal of Geophysical Research: Atmospheres, 116, n/a–n/a, doi:10.1029/2010JD015373, 2011b.

Pongratz, J., Reick, C., Raddatz, T., and Claussen, M.: A reconstruction of global agricultural areas and land cover for the last millennium, Global Biogeochemical Cycles, 22, n/a–n/a, doi:10.1029/2007GB003153, gB3018, 2008.

Press, W., Flannery, B., Teukolsky, S., and Vetterling, W.: Numerical Recipes in Fortran 77: The Art of Scientific Computing, Cambridge University Press, 1992.

Raddatz, T., Reick, C., Knorr, W., Kattge, J., Roeckner, E., Schnur, R., Schnitzler, K.-G., Wetzel, P., and Jungclaus, J.: Will the tropical land biosphere dominate the climate-carbon cycle feedback during the twenty-first century?, Climate Dynamics, 29, 565–574, doi:10.1007/s00382-007-0247-8, 2007.

Raupach, M. R., Rayner, P. J., Barrett, D. J., DeFries, R. S., Heimann, M., Ojima, D. S., Quegan, S., and Schmullius, C. C.: Model–data synthesis in terrestrial carbon observation: methods, data requirements and data uncertainty specifications, Global Change Biology, 11, 378–397, doi:10.1111/j.1365-2486.2005.00917.x, 2005.

Rayner, P. J., Enting, I. G., Francey, R. J., and Langenfelds, R. L.: Reconstructing the recent carbon cycle from atmospheric CO_2, $\delta^{13}C$ and O_2/N_2 observations, Tellus, 51B, 213–232, 1999.

Rayner, P. J., Scholze, M., Knorr, W., Kaminski, T., Giering, R., and Widmann, H.: Two decades of terrestrial carbon fluxes from a carbon cycle data assimilation system (CCDAS), Global Biogeochem. Cycles, 19, GB2026–, 2005.

Reick, C. H., Raddatz, T., Brovkin, V., and Gayler, V.: Representation of natural and anthropogenic land cover change in MPI-ESM, Journal of Advances in Modeling Earth Systems, 5, 459–482, doi:10.1002/jame.20022, 2013.

Rödenbeck, C., Houweling, S., Gloor, M., and Heimann, M.: CO_2 flux history 1982–2001 inferred from atmospheric data using a global inversion of atmospheric transport, Atmospheric Chemistry and Physics, 3, 1919–1964, doi:10.5194/acp-3-1919-2003, 2003.

Rödenbeck, C., Keeling, R. F., Bakker, D. C. E., Metzl, N., Olsen, A., Sabine, C., and Heimann, M.: Global surface-ocean p^{CO_2} and sea–air CO_2 flux variability from an observation-driven ocean mixed-layer scheme, Ocean Science, 9, 193–216, doi:10.5194/os-9-193-2013, 2013.

Roeckner, E., Bäuml, G., Bonaventura, L., Brokopf, R., Esch, M., Giorgetta, M., Hagemann, S., Kirchner, I., Kornblueh, L., Manzini, E., Rhodin, A., Schlese, U., Schulzweida, U., and Tompkins, A.: The atmospheric general circulation model ECHAM5 - Part 1: model description, Report 349, Max-Planck Institute for Meteorology, Hamburg, ISSN 0937 - 1060, 2003.

Saito, M., Ito, A., and Maksyutov, S.: Optimization of a prognostic biosphere model for terrestrial biomass and atmospheric CO_2 variability, Geoscientific Model Development, 7, 1829–1840, doi:10.5194/gmd-7-1829-2014, 2014.

Saugier, B. and Roy, J.: Estimations of Global Terrestrial Productivity: Converging Towards a Single Number?, in: Global Terrestrial Productivity: Past, Present and Future, edited by Mooney, H., Roy, J., and Saugier, B., Academic Press, San Diego, 2001.

Schneck, R., Reick, C. H., and Raddatz, T.: Land contribution to natural CO2 variability on time scales of centuries, Journal of Advances in Modeling Earth Systems, 5, 354–365, doi:10.1002/jame.20029, 2013.

Scholze, M., Kaminski, T., Rayner, P., Knorr, W., and Giering, R.: Propagating uncertainty through prognostic carbon cycle data assimilation system simulations, J. Geophys. Res., 112, D17 305–, 2007.

Sitch, S., Huntingford, C., Gedney, N., E., L. P., Lomas, M., Piao, S. L., Betts, R., Ciais, P., Cox, P., Friedlingstein, P., Jones, C. D., Prentice, I. C., and Woodward, F. I.: Evaluation of the terrestrial carbon cycle, future plant geography and climate-carbon cycle feedbacks using five Dynamic Global Vegetation Models (DGVMs), Global Change Biology, 14, 2015–2039, doi:10.1111/j.1365-2486.2008.01626.x, 2008.

Sitch, S., Friedlingstein, P., Gruber, N., Jones, S. D., Murray-Tortarolo, G., Ahlström, A., Doney, S. C., Graven, H., Heinze, C., Huntingford, C., Levis, S., Levy, P. E., Lomas, M., Poulter, B., Viovy, N., Zaehle, S., Zeng, N., Arneth, A., Bonan, G., Bopp, L., Canadell, J. G., Chevallier, F., Ciais, P., Ellis, R., Gloor, M., Peylin, P., Piao, S. L., Le Quéré, C., Smith, B., Zhu, Z., and Myneni, R.: Recent trends and drivers of regional sources and sinks of carbon dioxide, Biogeosciences, 12, 653–679, doi:10.5194/bg-12-653-2015, 2015.

Voßbeck, M., Clerici, M., Kaminski, T., Lavergne, T., Pinty, B., and Giering, R.: An inverse radiative transfer model of the vegetation

canopy based on automatic differentiation, Inverse Problems, 26, 095 003, 2010.

Weedon, G. P., Balsamo, G., Bellouin, N., Gomes, S., Best, M. J., and Viterbo, P.: The WFDEI meteorological forcing data set: WATCH Forcing Data methodology applied to ERA-Interim reanalysis data, Water Resources Research, 50, 7505–7514, doi:10.1002/2014WR015638, 2014.

Williams, M., Richardson, A. D., Reichstein, M., Stoy, P. C., Peylin, P., Verbeeck, H., Carvalhais, N., Jung, M., Hollinger, D. Y., Kattge, J., Leuning, R., Luo, Y., Tomelleri, E., Trudinger, C. M., and Wang, Y. P.: Improving land surface models with FLUXNET data, Biogeosciences, 6, 1341–1359, doi:10.5194/bg-6-1341-2009, 2009.

Zaehle, S., Sitch, S., Smith, B., and Hatterman, F.: Effects of parameter uncertainties on the modeling of terrestrial biosphere dynamics, Global Biogeochemical Cycles, 19, n/a–n/a, doi:10.1029/2004GB002395, gB3020, 2005.

Ziehn, T., Scholze, M., and Knorr, W.: On the capability of Monte Carlo and adjoint inversion techniques to derive posterior parameter uncertainties in terrestrial ecosystem models, Global Biogeochemical Cycles, 26, n/a–n/a, doi:10.1029/2011GB004185, http://dx.doi.org/10.1029/2011GB004185, gB3025, 2012.